Dept. of Anatomy and Histology,
Faculty of Veterinary Medicine, Assiut University, Assiut, Egypt

QUANTITATIVE HISTOCHEMICAL STUDY ON THE POSTNATAL DEVELOPMENT OF PERINEURONAL NETS IN THE RETROSPLENIAL CORTEX OF ALBINO RATS

(With 4 Tables and 19 Figures)

By

R. SAYED

(Received at 10/3/2009)

دراسة هستوكيميائية كمية على تطور الأغلفة العصبونية الشبكية بالقشرة الطحالية الخلفية لمخ الجرذان البيضاء في فترة ما بعد الولادة

رمضان سيد

يتميز الجهاز العصبي المركزي للثدييات والزواحف والأسماك بوجود معاطف شبكية الشكل، تسمى الأغلفة العصبونية الشبكية، وهذه الأغلفة غنية بجزيئات البروتوجليكانز أو الجليكوبروتين أو مزيج الاثنين معاً، حيث تغلف أسطح خلايا بعض الدوائر العصبية. تم في هذه الدراسة فحص الخصائص الهستوكيميائية الكمية للأغلفة العصبونية وكذلك تطورها بالقشرة الطحالية الخلفية لمخ الجرذان البيضاء في فترة ما بعد الولادة، وذلك باستخدام صبغة الحديد الغروي (CIC) أو بعد تنشيطها بنترات الفضة (CIC/Bodian's) وذلك لتوسيم جزيئات البروتوجليكانز المكبرتة، وأيضاً تم استخدام بعض اللكتينات النباتية مثل (VVA، WFA ، SBA) لتمييز جزيئات الجليكوبروتين. وقد ظهرت الأغلفة العصبونية لأول مرة في الجرذان التي بلغت أعمارها 1-2 أسبوع بعد الولادة حول بعض العصبونات المنتشرة بالطبقات القشرية الخامسة حتى الثانية، وأبدت العصبونات المغلفة زيادةً مطردة في أعدادها، وكثافتها الاصطباغية بتقدم العمر. وعند بلوغ الجرذان عمر 5 أسابيع ظهرت الأغلفة العصبونية بهيئة محددة، وأمكن تمييزها إلى أغلفة مكونة من البروتوجليكانز أو الجليكوبروتين أو أغلفة مختلطة من البروتوجليكانز والجليكوبروتين. أظهرت الدراسات الكمية أن الكثافة العددية الكلية للعصبونات المغلفة كانت 1.80 ± 0.29 بوحدة المساحة (60.15 ميكرون مربع) في الجرذان التي بلغت أعمارها أسبوعان، وذلك باستخدام الصبغة المزدوجة (WFA/CIC)، وأبدت هذه الخلايا زيادةً معنوية جداً بتقدم العمر، حيث وصلت أعدادها إلى 9.12 ± 1.82 بوحدة المساحة عند بلوغ عمر الجرذان 12 أسبوعاً، وتبين من التحاليل الإحصائية الكمية أن العصبونات المغلفة تضاعفت 2.86 مرة خلال الشهر الأول، بينما ازدادت 1.73 مرة خلال الشهر الثاني، و1.02 مرة خلال الشهر الثالث بعد الولادة. وأظهرت التحاليل الإحصائية أن الخلايا العصبونية المغلفة بالبروتوجليكانز والجليكوبروتين أو ذات الغلاف المختلط أبدت زيادة معنوية جداً بتقدم عمر الحيوانات خلال الشهور الثلاثة الأولى بعد الولادة. وأظهرت التحاليل القياسية أن الكثافة العددية المطلقة للعصبونات المغلفة والتي تم

توسيمها بصبغة VVA، WFA، SBA، CIC، CIC-Bodian's في الحيوانات التي بلغت أعمارها أسبوعان كانت 0.17±2.12 ، 0.13±1.80 ، 0.00 ، 0.00 ، 0.18±3.00 بوحدة المساحة على التوالي، ثم ازدادت القيم السابقة بتقدم العمر وكانت الزيادة معنوية جداً، حيث وصلت كثافتها العددية بوحدة المساحة إلى 1.23±6.13 ، 1.03±5.00 ، 0.69±2.90 ، 0.76±3.85 ، 1.13±4.30 على التوالي. وكان معامل التوسيم للخلايا العصبونية الموسمة بالصبغات السابقة في الحيوانات التي بلغت أعمارها أسبوعان هو 3.60, 3.52 ,0.00 ,0.00 ,2.94على التوالي ، ثم ازدادت هذه المتغيرات بتقدم العمر وبلغت نسبتها في الحيوانات التي بلغت أعمارها 12 أسبوعاً 11.02 ,9.87 ,7.43 ,12.82 ,15.84، على التوالي، وكانت الزيادة معنوية جداً. وقد أوضحت الدراسة الحالية أن تطور الشبكات العصبونية بالقشرة الطحالية الخلفية لمخ الجرذان البيضاء ارتبط ارتباطاً معنوياً بتقدم العمر، وقد يرتبط ظهورها بالهجرة الخلوية ، أو النضج الوظيفي للخلايا العصبونية المغلفة. والنتائج الحالية تقدم قاعدة بيانات أساسية يمكن أن يعتمد عليها في الدراسات المستقبلية التجريبية أو البيئية المنوطة بالقشرة الطحالية الخلفية للجرذان البيضاء والتي قد تتوسع لتشمل الثدييات الأخرى ومتضمنة الجنس الآدمي.

SUMMARY

Reticular or lattice-like perineuronal coatings of condensed extracellular matrix (ECM), termed perineuronal nets (PNs), enriched in proteoglycans (PGs) and/or glycoproteins (GPs) were demonstrated to ensheath cell surfaces of certain neuronal circuits in the central nervous system (CNS) of mammals, reptiles and fishes. In the present study, the histochemical and quantitative characteristics of postnatal ECM in the retrosplenial cortex (RSC) of albino rats were described with a cationic iron colloid (CIC) or with CIC-Bodian's technique for detection of sulfated PGs and with certain plant lectins from *Vicia villosa* agglutinin (VVA), *Wisteria floribunda* agglutinin (WFA) or *Glycine max* agglutinin (SBA) for demonstration of *N*-acetylgalactosamine containing GPs. The differentiating PNs were shown to make their development as early as 1-2 weeks postnatally (Pw1-2), which surround the surface of some neurons distributing throughout the II-V cortical layers. During the first postnatal month and onwards, the net-encapsulated neuronal cells underwent progressive increment in number and presented an inside-out pattern of migration and differentiation throughout the V-II cortical layers. At a later stage (Pw6-8), the overall density and intensity of labeled PNs progressively increased and reached the adult stage of development. In addition, they displayed their differential labeling characteristics for the lectin/CIC double staining, which were differentially identified into three types, namely; PGs-, GPs-, and PGs/GPs coats. The morphometric investigation revealed that the total

density of net-associated retrosplenial neurons (RSNs) at Pw2 was about 1.80±0.29 /UA (UA = 60.15 μm^2) after labeling with the WFA/CIC double staining technique, and this variant increased polynomially with progression of postnatal age reaching 9.12±1.82 /UA at Pw12. Quantitative analysis showed that the gain of net-associated RSNs increased rapidly during the first postnatal month (2.86 fold), and then increased 1.73 fold during the second month, but increased 1.02 fold at the third month. Statistical analysis revealed that throughout the postnatal period, the numerical density of net-associated RSNs increased significantly with advance of age (R = +0.992; P<0.01). In addition, the numerical densities of PGs- and GPs-coated neurons, as well as those exhibiting coat complexes (PGs/GPs coats), increased polynomially with progression of animal age (R = +0.996, +0.990 and +0.976, respectively with P < 0.01 in all parameters). At Pw2, the absolute numerical density of RSNs labeled with VVA, WFA, SBA, CIC and CIC-Bodian's staining measured about 2.12±0.17, 1.80±0.13, 0.00, 0.00 and 3.00±0.18 /UA, respectively. These parameters increased significantly with postnatal age and respectively reached 6.18±1.23, 5.00±1.03, 2.90±0.69, 3.85±0.76 and 4.30±1.13 /UA at Pw12 (R = +0.995, +0.995, +0.997, +0.996 and 0.984 with P<0.01 for all parameters). In addition, labeling indices of RSNs stained with the aforementioned staining at Pw2 was 3.60, 2.94, 0.00, 0.00 and 3.52, respectively. These variants increased significantly with advance of animal age reaching 15.84, 12.82, 7.43, 9.87 and 11.02, respectively (R = +0.994, +0.997, +0.998, +0.996 and +0.999 and P< 0.01 for all variants). This finding indicated that the perineuronal ECM components are significantly correlated with age and suggest a possible developmental and biological significance including promotion of migration and functional maturation of net-associated neurons in the RSC. In addition, the finding of present study would be contributed as baseline for future experimental or environmental studies that are expandable for other mammalian species including the human.

Key words: *Quantitative study, Perineuronal nets, Glycoproteins, Proteoglycans, Retrosplenial cortex*

INTRODUCTION

The extracellular matrix of brain is mainly present in the intercellular spaces between neurons and glial cells. This matrix is first described by Camilo Golgi and Santiago Ramón y Cajal, late in the 19th century, when iron and silver impregnation techniques allowed them to

visualize the perineuronal nets (Celio *et al.,* 1998; Yamaguchi, 2000). Whereas most of this matrix is amorphous, there are specialized structures of dense organized matrix (PNs) around certain neuronal subpopulations with holes at the sites of synaptic contacts (Celio and Blümcke 1994; Celio *et al.,* 1998). The PNs ensheath the neuronal soma, proximal parts of dendrites, as well as the axon initial segment, thus surrounding all presynaptic buttons attached to these structures (Hendry *et al.,* 1988; Brückner *et al.,* 1993). Adjacent astrocytic processes usually dip into the matrix material (Atoji and Suzuki, 1992; Brückner *et al.,* 1993), thereby forming an outer, glial, part of PNs (Brauer *et al.,* 1984). Proteoglycans and glycoproteins are among the main ECM components of the CNS in mammals (Matsui *et al.,* 1999; Yamaguchi 2000).

The major ECM constituents of PNs have been characterized as chondroitin sulfate proteoglycans (CS-PGs) that are members of the aggrecan-versican-neurocan-brevican family of PGs (Brückner *et al.,* 1994; Yamaguchi, 2000). These PGs usually occur complexed with hyaluronan (HA) (Bignami *et al.,* 1992; Köppe *et al.,* 1997b) and/or with GPs (Yamaguchi 2000; Sayed *et al.,* 2002), and anchored to the neuronal surface via certain link proteins. In addition, CS-PGs phosphacans was shown to be associated with PNs in the rat cerebral cortex. To date, four members of the tenascin family of GPs, namely; tenascin-C (Tn-C) (Celio and Chiquet-Ehrismann, 1993), tenascin-R (Tn-R) (Wintergerst *et al.,* 1996), as well as Tn-W and Tn-X (Costa *et al.,* 2007), which were immunocytochemically detected as constituents of PNs. Therefore, the PNs are differentially identified into three varieties according to their molecular composition, namely; proteoglycans coats, glycoproteins coats and coat complexes, formed of PGs networks intermingled with GPs molecules (Sayed *et al.,* 2002). There is evidence that these structures are involved in the regulation of neuronal plasticity (Hockfield *et al.,* 1990; Pizzorusso *et al.,* 2002), in neuroprotection (Brückner *et al.,* 1999; Morawski *et al.,* 2004), and in support of ion homeostasis around highly active neurons (Brückner *et al.,* 1993, Hartig *et al.,* 1999). In addition, PNs are thought to be associated with fast-spiking types of neurons and streams of rapid information processing (Kawaguchi *et al.,* 1987).

During postnatal development, ECM molecules progressively accumulate around somatic and dendritic synapses of certain neurons, contributing to the formation of the perineuronal nets (Celio *et al.,* 1998). These specialized ECM structures appear to restrict plasticity in

adults, and their appearance corresponds with the end of critical period of plasticity. In addition, as the CNS matures the level of plasticity declines. Notably, the appearance of PNs in some brain regions (e.g. visual cortex) can be delayed by dark rearing, which prolongs plasticity (Deepa *et al.,* 2006). However, degradation of CS-GAGs (chondroitin sulfate glycosaminoglycans) constituent of PNs restores experience-dependent plasticity to adults (Celio *et al.,* 1998; Laabs *et al.,* 2005).

PNs develop, relatively late in the postnatal age (2-5 weeks postnatally) in a variety of mammals during the periods characterized by synaptic refinement, myelination, and acquisition of an adult-like pattern of physiological activity (Bignami *et al.,* 1992; Wintergerst *et al.,* 1996; Köppe *et al.,* 1997a). Their time of appearance and maturation corresponds with the development of the mature neuronal phenotype, as well as termination of plasticity at the end of critical periods of many parts of CNS (Hockfield *et al.,* 1990). In mice, the first PNs in the cerebral cortex appear after the second postnatal week as shown by specific lectin staining. However, PNs associated with neurons in the subcortical nuclei develop earlier (Nakagawa *et al.,* 1987; Murakami *et al.,* 1997).

CS-PGs in the CNS can interact with various growth factors and cell adhesion molecules, playing a significant role in development (Oohira *et al.,* 2000). They mostly have an inhibitory effect toward neurite outgrowth and regeneration, either via their chondroitin sulfate chains or core proteins (Rhodes *et al.,* 2004). However, ECM glycoprotein tenascin-R has been implicated in the control of axon targeting, neural cell adhesion, migration and differentiation, and matrix assembly in PNs together with maintenance of their integrity in adults (Brenneke *et al.,* 2004). Interestingly, the PNs are up-regulated after CNS injury, and the enzymatic removal of glycosaminoglycan (GAG) chains from CS-PGs with chondroitinase ABC improves axon regeneration and functional recovery (Bradbury *et al.,* 2002).

Although the net-associated neurons constituted a considerable population in CNS, their histochemical and functional significance is still obscure. Therefore, one approach of elucidating their possible biological significance is to monitor their development and to indicate their histochemical and quantitative features in order to correlate such data to certain functional features.

The markers used in the present study for the demonstration of PNs-enriched with GPs are the plant lectins from *Vicia villosa* agglutinin (VVA, Nakagawa *et al.,* 1986), *Wisteria floribunda* agglutinin (WFA,

Härtig *et al.*, 1992), *Glycine max* agglutinin (SBA, Lüth *et al.*, 1992). However, a cationic iron colloid (Brauer *et al.*, 1984; Murakami *et al.*, 1986; Brückner *et al.*, 1993) and/or CIC/Bodian's staining (Murakami *et al.*, 1997) was applied for demonstration of PNs with sulfated PGs. In addition to these markers we have used the CIC method after lectin labeling in order to differentially label sulfated PGs and unsulfated glycoconjugates components (GPs) of ECM (Murakami *et al.*, 1995). All of the above mentioned markers have been proven to be sensitive tools for demonstration of PNs.

The present study was undertaken (i) to demonstrate patterns of development of PNs, and (ii) to reveal certain histochemical and morphometric data on PNs in the RSC and the obtained data are presented in form of tables and developmental curves. The granular and non-granular subfields of rat RSC were used for this study as it contains many neurons associating with well developed pericellular coats (Sayed *et al.*, 2002). This cortex is involved in navigation and processing of episodic memory (Maguire 2001), as well as acquisition or extension of the trace conditioned reflex (Weible *et al.*, 2000). Therefore, the present investigation systematically supplements our previous studies of PNs in the RSC of rats. Analysis of the postnatal development of RSC, as well as identification of its histochemical and morphometric characteristics is likely to provide an essential basis for understanding its functioning in the CNS of mammals as well.

MATERIALS and METHODS

1. Animals and tissue processing

The material for this investigation originated from 122 Wistar rats, of both sexes, ranging from 0-day (PD0) to 12-weeks-old (Pw12). Treatment of animals was in accordance with the Ethical guidelines of the Okayama University, Japan. Wistar rats at birth (n= 6) and postnatal weeks 1 (Pw1) (n= 10), 2 (n= 10), 3 (n= 10), 4 (n= 12), 5 (n= 12), 6 (n= 12), 7 (n= 12), 8 (n= 12), 10 (n= 12), as well as 12 weeks-old animals (n= 12) were perfused transcardially under deep ether anesthesia with saline, followed by 4% paraformaldehyde in 0.1 M sodium cacodylate buffer (pH 7.3). The brains were isolated and 2-3 mm-thick tissue slices traversing the granular and agranular subfields of retrosplenial cortex were cut in saggital or coronal planes and immersed in the aforementioned fixative.

After fixation, specimens were dehydrated, cleared and embedded in paraffin. Serial saggital and coronal sections (5-7 µm in thickness) were prepared and after deparaffinization by xylene they were treated as follows:

2. Histochemistry and cytochemistry

2.1. Colloidal iron histochemistry

To estimate the development of polyaninonic components (sulfated PGs) incorporated into the ECM, tissue sections were incubated with a cationic iron colloid at pH 1.5 (Murakami *et al.*, 1986) and the reaction was demonstrated by Prussian blue. Counter staining with nuclear fast red was inserted prior to balsam embedding. Sections for control were not treated with iron colloid, but were subjected to the Prussian blue reaction.

2.2. Lectin cytochemistry

Brain tissue sections were incubated with lectin Vicia villosa agglutinin (Kosaka and Heizmann, 1989), lectin *Wisteria floribunda* agglutinin (Härtig *et al.*, 1992), as well as lectin *Glycine max* agglutinin (Lüth *et al.*, 1992). The aim was to examine the temporo-spatial distribution pattern of N-acetylgalactosamine (*Gal*NAc) containing glycoconjugates (GCs) (Table: 1). Peroxidase activity was visualized with 3,3´-diaminobenzidine tetrahydrochloride. Counter staining with Mayer's hematoxyline was inserted prior to balsam embedding. Controls for lectin-stained sections were consisted of adjacent sections and treated with phosphate buffer containing no agglutinin.

2.3. Dual staining of lectin- labeled sections with CIC

Some sections were stained with WFA, VVA or SBA and then doubled with a cationic iron colloid. The aim was to allow differentiation and temporo-spatial distribution of sulfated PGs and unsulfated *Gal*NAc containing glycoconjugates.

2.4. Doubling of CIC-stained sections with Bodian's procedure

The combined staining of CIC with Bodian's technique would allow precise visualization for the differentiating sulfated proteoglycans nets (Murakami *et al.*, 1997).

3. Photography

All stained preparations were examined with a transmission light microscope (Olympus BX 50 or BH2). Photographic documentation was performed by using Kodak TM color film and presented on their original magnifications.

4. Histomorphometry and Stereology

The stained sections were quantitatively analyzed under a light microscope using an eye piece graticule (400X magnification) (Weibel, 1979) and computer adjusted image analysis system (Leica Q500 MC Program). All stained sections were used for measuring the following parameters:

1. Number (density) of net-associated (coated) neurons, non-coated neurons and the total neuronal number per unit area (UA, 60.15 µm2) [estimated from WFA/CIC stained sections of all age groups]. The mean values (absolute numerical densities) measured from each age group were used to calculate the relative densities (percentage) of variables.
2. Relative densities of each type of coated neurons (PGs-coated neurons, GPs-coated ones and neurons exhibiting GPs/PGs coat complexes) [estimated from VVA/CIC, WFA/CIC and SBA/CIC stained sections of all age groups].
3. Absolute densities of net-associated neurons [estimated from the VVA, WFA, SBA, CIC and CIC/Bodian's stained sections of all age groups].
4. Labeling indices of VVA, WFA, SBA, CIC and CIC/Bodian's staining [estimated from the VVA, WFA, SBA, CIC and CIC/Bodian's stained sections of all age groups]. The labeling index of each stain was calculated from the number of labeled neurons by this stain, divided by the total number of neurons scored, and multiplied by 100.

The data were obtained for an average of about 36-58 randomly selected fields occupied by the differentiating retrosplenial nerve cells. Although tissue shrinkage is known to occur following similar tissue processing techniques, no specific estimation of this shrinkage was made in the present study and all obtained data were presented in relative units.

5. Statistical Analysis

Data obtained from the histomorphometric measurements were presented as means ±SD (standard deviation). Mean of variables were processed in an analysis of correlation and regression (one-way variance) to characterize the relationship between parameters evaluated (Weber, 1980). MRE (maximum relative error) of each variable was calculated from the estimated value that subtracted from the calculated value (from regression equation), divided by the estimated value, and then multiplied by 100. Values of $P<0.05$ were considered significant, and those <0.01 were highly significant.

RESULTS

1. Control experiments

In all treatments, control incubations resulted in a significant failure of the labeling (not shown).

2. General histochemical findings

The histochemical findings of postnatal development of the ECM components in the RSC of albino rats were presented in Fig. 1A-D.

In newborn animals the loose and condensed form of the ECM was failed to be revealed by all markers used in this investigation. The first detection of labeled perineuronal ECM molecules was revealed at the end of the first postnatal week, around few sporadic neurons distributing in layer V and IV, by using lectin WFA and VVA, as well as by the CIC-Bodian's procedure. During postnatal development the labeled or net-associated retrosplenial neurons gradually increased in number and presented radial inside-out pattern of differentiation and migration throughout the layers of RSC. The labeling intensity of perineuronal ECM molecules was weak to moderate during the second and third postnatal weeks, and then gradually increased with progressing of age toward maturity. With advancement of postnatal age, the continuous accumulation of ECM molecules resulted in gradual increment of staining intensity and thickening of differentiating perineuronal sheaths, as well as recent development of PNs around further neurons (Fig. 1A-D). Therefore, the deposition of matrix molecules in PNs and intervening neuropil appeared to be a continuous process and not transient in nature.

Between Pw4-5, an immature staining of perineuronal sheaths was attained around several neurons distributing in the V-II layers (Fig. 1A). Onwards, the morphological maturation or the appearance of adult-like form of matrix components accumulating in PNs or intervening neuropil was reached at Pw6-8 (Figs. 1C-1D). The net-associated neurons in the adult rats of present study were distributed mainly in layer IV and II, but appeared to be fewer in number in layer V and III (Figs. 1C and 1D). Furthermore, the PNs were associated mainly with the non-pyramidal cells (interneurons), but to a lesser extent with the pyramidal ones (Figs. 1C-1D). These PNs varied in thickness and staining intensity from cell to another, which was thicker, sharper and intensely stained around the non-pyramidal neurons, however, they were thin, less sharp and faintly stained around the pyramidal ones (Figs. 1C and 1D).

Notably, the commencement of ECM labeling with the CIC or lectin SBA staining was demonstrated for the first time during the fourth postnatal week. In addition, the first indication of differential labeling of developing PNs was also expressed at this developmental period by using the lectin-CIC double labeling experiment. Therefore, after using this dual staining procedure the PNs appeared to be either solely stained with CIC (blue, PGs-enriched PNs), or labeled with lectins (yellow, GPs-enriched PNs) and/or stained doubly with CIC and lectin (greenish to dark-brown, PGs/GPs-enriched PNs). The CIC/Bodian's staining of PGs-enriched PNs was sharp and showed a relatively higher labeling intensity (Fig. 1C) than those solely stained with the CIC staining (Fig. 1B). The morphological features, distribution, as well as staining pattern of lectin labeled PNs were similar to those labeled by the CIC or CIC-Bodian's (Fig. 1A-1D). However, labeling intensity of lectin-labeled GPs-enriched sheaths and intervening neuropil differed considerably with respect to the lectin used. This variant was much intense in sections treated with lectin VVA and WFA than those treated with SBA. In addition, the intensity of PGs/GPs coats (coat complexes) varied considerably among lectins, which appeared with higher intensity in sections stained with VVA/CIC and WVA/CIC staining than those stained by SBA/CIC.

3. Quantitative histochemical findings

The histochemical characteristics and quantitative parameters of the RSC in albino rats and their relation to the postnatal age were presented in Tables 2-4 and Figs. 2-19.

3.1. Total density of retrosplenial neurons

Quantitative analysis of the postnatal RSC in albino rats revealed that the mean number of total retrosplenial neurons at the first postnatal week was about 46.33±2.3 /UA, and this parameter gradually decreased with advance of postnatal age reaching 39.10±3.13 at Pw12 (Table 2 and Figs. 2, 3). Throughout the postnatal period the correlation between the total neuronal density and animal age was polynomially well expressed and highly significant ($R = -0.985$; $P<0.01$) (Fig. 3). The calculated maximal relative error (MRE) from regression equation was about 1.39%.

3.2. Density and percentage of non-coated retrosplenial neurons

3.2.1. Density of non-coated retrosplenial neurons

The numerical density of non-coated RSNs as revealed by the WFA-CIC staining at Pw2 was about 43.21±3.43 /UA (Table 3). This variant showed gradual decrease with progression of postnatal age,

reaching 29.98±3.23 /UA at Pw12 (Table 3 and Fig. 2). The polynomial regression curve was best described and fitted the data (R = -0.991; P<0.01; MRE = 2.51%) better than the logarithmic or exponential curves (Fig. 4).

3.2.2. Percentage of non-coated retrosplenial neurons

The percentage or relative density of non-coated RSNs in rats of 2-weeks old was about 95.72% of the total neuronal population. This ratio underwent gradual decrease with advance of postnatal age reaching 76.68% at Pw12 (Table 3).

3.3. Density and percentage of net-associated retrosplenial neurons

3.3.1. Density of net-associated retrosplenial neurons

Density of coated or net-associated RSNs in rats of 2-weeks old measured 1.8±0.29 /UA as estimated from the WFA-CIC stained sections (Table 3 and Fig. 2). This variable progressively increased with advance of animal age reaching 5.16±1.62 /UA at Pw4 and then showed slow steady increase with advance of age, reaching 9.12±1.82 at Pw12. Therefore, the gain of net-associated RSNs increased rapidly during the first postnatal month (2.86 fold), and then increased 1.73 fold during the second month, but increased 1.02 fold during the third postnatal month. Throughout the postnatal period the correlation between the numerical density of net-associated RSNs and animal age was well expressed and highly significant (R = +0.992; P<0.01; MRE = 12.96%) (Figs. 2 and 5).

3.3.2 Percentage of net-associated retrosplenial neurons

The percentage or relative density of coated RSNs in rats of 2-weeks old was about 4.28% as determined from the WFA-CIC stained sections (Table 3). This variant presented gradual increase with progression of postnatal age coinciding with the decrement of the percentage of non-coated neurons (Table 3). On reaching Pw12 the percentage of the coated to non-coated neurons was about 23.32%: 76.68% (Table 3).

3.4. Differential densities of net-associated retrosplenial neurons

Investigation of the postnatal RSC of rats using the dual WFA/CIC, VVA/CIC and SBA/CIC staining revealed three types of net-associated neurons: GPs-, PGs- and PGs/GPs-coated neurons. The differential labeling presented by the aforementioned dual staining procedure was detected for the first time at the fourth postnatal week (Table 3 and Fig. 6).

3.4.1. Density of PGs- coated retrosplenial neurons

Density of net-associated neuronal cells whose extracellular coats enriched with PGs molecules (PGs coats) as revealed with the

WFA/CIC staining was about 0.2±0.02 /UA in rats of 8-weeks old (Table 3). This variable underwent slow gradual increase with advance of animal age reaching 0.5±0.18 at Pw12 (Table 3 and Fig. 6). The polynomial regression line was best described and fitted the data (R = +0.996; P<0.01; *MRE* = 17%) better than the logarithmic or exponential curves (not shown).

3.4.2. Density of GPs- coated retrosplenial neurons

In rats of 2-weeks old, the mean number of net-associated RSNs whose coats enriched with GPs molecules (GPs coats) was about 1.8±0.29 /UA as revealed with the WFA/CIC staining (Table 3). This variant progressively increased (3.4 fold) with advance of age, reaching 6.20±1.32 /UA at Pw8, thereafter the value was about 6.06±1.82 and 6.10±1.82 in rats of Pw10 and Pw12, respectively (Table 3 and Figs. 6, 7). Throughout the postnatal period the GPs-coated RSNs increased polynomially with advance of animal age (R = +0.990; P<0.01; MRE = 15.1%) (Fig. 7).

3.4.3. Density of PGs/GPs- coated retrosplenial neurons

The numerical density of PGs/GPs-coated RSNs was about 1.71±0.32 /UA in rats of 4-weeks old (Table 3). This parameter underwent slow gradual increase with progression of age, reaching 2.53±0.84 /UA at Pw8, and thereafter the value was fluctuated between 2.51±0.87 and 2.52±0.92 at Pw10 and Pw12, respectively (Table 3 and Fig. 6). Between Pw4 and Pw12 the PGs/GPs-coated RSNs increased polynomially with progression of postnatal age (R = +0.976; P<0.01; MRE = 5%) (not shown).

3.5. Absolute labeling densities of RSNs stained with VVA, WFA, SBA, CIC or CIC/Bodian's staining

The absolute labeling densities of RSNs stained with VVA, WFA, SBA, CIC and CIC/Bodian's staining were presented in Table 2 and Figs. 8-13. Notably, quantitative histochemical analysis of the postnatal RSC in rats showed significant developmental criteria including the intensity, heterogeneity, as well as density of labeled neuronal cells by the aforementioned markers.

3.5.1. Absolute density of VVA- labeled neurons

The signaling of VVA labeling in the ECM of rat RSC was detected, for the first time, at the end of the first postnatal week. At Pw2, the absolute numerical density of VVA-labeled neuronal cells measured about 2.12±0.17 /UA (Table 2). This variable presented a progressive increment during the third and fourth postnatal weeks (2.56 fold), then presented a slow increase with advance of animal age,

reaching 6.18±1.23 /UA at Pw12 (Table 2 and Figs. 8 and 9). Throughout the investigated postnatal months, the non-linear polynomial regression line was best described (R = +0.995; P<0.01; *MRE* = 9%) and fitted the data better than the simple regression line and logarithmic or exponential curves (Fig. 9).

3.5.2. Absolute density of WFA- labeled neurons

The absolute numerical density of WFA-labeled RSNs was about 1.8±0.13 /UA at the second postnatal week (Table 2). This parameter underwent a progressive increase (2.22 fold) during the first postnatal month, and then showed slow steady increment with advance of age, reaching 5.00±1.03 /UA at Pw12 (Table 2 and Figs. 8 and 10). The polynomial regression curve was best described for the present data (R = +0.995; P<0.01; *MRE* = 10%) (Fig. 10).

3.5.3. Absolute density of SBA- labeled neurons

The SBA labeling was detected in the RSC of rats, for the first time, during the fourth postnatal week. At this developmental stage, the absolute numerical density of SBA- labeled RSNs measured about 0.50±0.12 /UA, then presented slow steady increase with advance of age, reaching 2.90±0.69 /UA at Pw12 (Table 2 and Figs. 8, 11). During the second and third postnatal month the absolute density of SBA-labeled neurons increased polynomially with progression of age (R = +0.997; P<0.01; *MRE* = 9%) (Fig. 11).

3.5.4. Absolute density of CIC- labeled neurons

The signaling of CIC stain in the RSC of rats was detected, for the first time, at the fourth postnatal week and that the CIC-labeled cells at this developmental age measured about 1.12±0.16 /UA (Table 2 and Figs. 8, 12). During the second postnatal month the CIC- labeled neurons underwent a progressive increase (3.85 fold), and then presented slow steady increase in the third month, reaching 3.85±0.76 at Pw12. The correlation of absolute neuronal density with postnatal age was well expressed and highly significant (R = +0.996; P<0.01; *MRE* = 23%) (Fig. 12).

3.5.5. Absolute density of CIC/Bodian's- labeled neurons

Binding activity of the CIC-Bodian's staining to the PGs-coated neurons was detected at the seventh postnatal day. During the second postnatal week, the absolute numerical density of labeled RSNs measured about 3.00±0.18 /UA (Table 2 and Figs. 8 and 13). This variant presented a slow gradual increase with advance of postnatal age, reaching 4.30±1.13 /UA at Pw12 (Table 2). The polynomial regression

curve was best described for the data (R = +0.984; P<0.01; *MRE* = 17%) (Fig. 13).

3.6. Labeling indices of neuronal cell population stained with VVA, WFA, SBA, CIC or CIC/Bodian's staining

Labeling indices of net-associated retrosplenial neuronal cells indicated by the VVA, WFA, SBA, CIC and CIC/Bodian's staining were presented in Table 4 and Figs. 14-19. The differences between the scored indices were statistically significant (not shown).

3.6.1. Labeling index of VVA staining

The labeling index of VVA-stained RSNs was about 3.60 at the second postnatal week (Table 4 and Fig. 14). This parameter increased 3.55 fold during the first postnatal month, reaching 12.80 at Pw4, then showed slow steady increase (0.98 fold) during the second month reaching 14.57 at Pw8, but increased 1.08 fold during the third month reaching 15.84 at Pw12. The polynomial regression line was well expressed and fitted the data (R = +0.994; P<0.01; *MRE* = 6.9%) better than the simple regression line and exponential or logarithmic curves (Fig. 15).

3.6.2. Labeling index of WFA staining

The labeling index indicated by the WFA staining was about 2.94 at the end of the second postnatal week (Table 4 and Fig. 14). This variable increased 3.03 fold during the first postnatal month, reaching 8.91 at Pw4, then underwent slow steady increment (1.3 fold) during the second month reaching 11.61 at Pw8, but increased 1.1 fold during the third month reaching 12.82 at Pw12. The polynomial regression curve was best described for the data (R = +0.997; P<0.01; *MRE* = 18.96%) (Fig. 16).

3.6.3. Labeling index of SBA staining

The signaling of SBA labeling was first indicated at the fourth postnatal week. At this stage the labeling index of SBA-stained RSNs was about 1.11 (Table 4 and Fig. 14). This variable increased 5.42 fold with advance of postnatal age, reaching 6.02 at Pw8, and then underwent slow gradual increment (1.23 fold) during the third postnatal month reaching 7.43 at Pw12. The polynomial regression curve was well expressed for our data (R = +0.998; P<0.01; *MRE* = 11.28%) (Fig. 17).

3.6.4. Labeling index of CIC staining

The commencement of CIC signaling was detected during the Pw4. At this developmental age the labeling index of RSNs was 2.48 (Table 4 and Fig. 14). This parameter increased 3.51 fold during the second postnatal month reaching 8.71 at Pw8, then underwent slow

steady increase (1.13 fold) with age which measured 9.87 at Pw12. The polynomial regression curve was best described for the present data (R = +0.996; P<0.01; *MRE* = 4.8%) (Fig. 18).

3.6.5. Labeling index of CIC/Bodian's staining

The labeling index of CIC/Bodian's stained neurons in the RSC was 3.52 at the second postnatal week (Table 4 and Fig. 14). This variant progressively increased (2.46 fold) during the first postnatal month reaching 8.66 at Pw4, then showed slow steady increase (1.18 fold) with advance of age reaching 10.25 at Pw8, but increased 1.07 fold during the third month which measured 11.02 at Pw12. The polynomial regression curve was well expressed for the data (R = +0.999; P<0.01; *MRE* = 7.5%) (Fig. 19).

Table 1: Lectins used, their source and sugar specificities.

Lectin abbreviation	Source of lectin	Sugar specificity	Reference
SBA	Glycine max	Beta GalNAc Alpha GalNAc	Lüth *et al.* (1992)
VVA	Vicia villosa	Alpha GalNAc Beta GalNAc	Murakami *et al.* (1999)
WFA	Wisteria floribunda	Alpha GalNAc Beta GalNAc	Nakagawa *et al.* (1986)

Abbreviation: GalNAc, N-acetylgalactosamine.

Table 2: Total neuronal density and absolute densities of labeled neurons per unit area indicated by the VVA, WFA, SBA, CIC and CIC-Bodian's staining in the RSC of postnatal rats.

Serial N	Age	N of Animals	Total N of RS neurons/UA	VVA-labeled neurons/UA	WFA-labeled neurons/UA	SBA-labeled neurons/UA	CIC-labeled neurons/UA	CIC/Bodian's-labeled neurons/UA
1	0 Day	6	--	*	*	*	*	*
2	1 Week	10	46.33±2.34	--	--	*	*	--
3	2 Weeks	10	45.01± 3.13	2.12 ±0.17	1.80 ±0.13	*	*	3.00 ±0.18
4	3 Weeks	12	45.02 ± 3.53	3.55 ±0.71	3.58 ±0.65	*	*	3.50 ±0.61
5	4 Weeks	12	45.01 ±2.45	5.44 ±0.94	4.01 ±0.78	0.50 ±0.12	1.12 ±0.16	3.90 ±0.83
6	5 Weeks	12	44.01 ±4.25	5.81 ±1.05	4.31 ±0.96	1.14 ±0.15	2.13 ±0.25	4.20 ±0.86
7	6 Weeks	12	43.00 ±3.36	6.00 ±1.10	4.60 ± 006	1.66 ±0.26	3.11 ±0.59	4.29 ±0.88
8	7 Weeks	12	42.01 ±3.75	6.08 ±1.21	4.80 ±1.02	2.01 ±0.36	3.54 ±0.81	4.30 ±0.97
9	8 Weeks	12	42.01 ±2.13	6.12 ±1.22	4.88 ±1.05	2.53 ±0.68	3.66 ±0.78	4.30 ±1.05
10	10 Weeks	12	41.00 ±2.34	6.15 ±1.21	4.90 ±1.04	2.68 ±0.58	3.80 ±0.82	4.31 ±1.04
11	12 Weeks	12	39.10 ±3.13	6.18 ±1.23	5.00 ±1.03	2.90 ±0.69	3.85 ±0.76	4.30 ±1.13
P value			0.001	0.001	0.002	0.001	0.001	0.003

Abbreviations: (*), not detected; (--), not estimated; N, number; Mean ±SD; RS, retrosplenial neurons. UA, (unit area, 60.15 μm^2).

Table 3: Density and percentage of coated and non-coated neurons, as well as densities of GPs-, PGs-, GPs/PGs-coated neurons in the retrosplenial cortex of postnatal rats revealed by WFA-CIC staining.

Serial N	Age	N of Animals	N of Non-coated RS neurons/UA	Percentage of Non-coated RS neurons	N of Coated RS neurons/UA	Percentage of Coated RS neurons	N of GPs - coated neurons/UA	N of PGs-coated neurons/UA	N of PGs/GPs-coated neurons/UA
1	0 Day	6	--	--	*	*	*	*	*
2	1 Week	10	--	--	--	--	--	*	*
3	2 Weeks	10	43.21 ± 3.43	95.72	1.80 ±.0.29	4.28	1.80 ±.0.29	*	*
4	3 Weeks	12	41.44 ± 4.60	91.27	3.58 ±0.19	8.73	3.58 ±0.19	*	*
5	4 Weeks	12	39.85 ± 3.02	87.42	5.16 ±1.62	12.58	3.45 ±1.09	*	1.71 ±0.32
6	5 Weeks	12	36.82 ± 4.53	82.03	7.19 ±1.72	17.97	5.00 ±1.12	*	2.19 ±0.35
7	6 Weeks	12	34.57 ± 3.16	78.93	8.43 ±1.70	21.07	6.01 ±1.22	*	2.42 ±0.67
8	7 Weeks	12	33.55 ± 2.75	78.85	8.46 ±2.02	21.15	6.00 ±1.25	*	2.46 ±0.79
9	8 Weeks	12	33.08 ± 4.51	77.68	8.93 ±1.82	22.32	6.20 ±1.32	0.2 ±0.02	2.53 ±0.84
10	10 Weeks	12	32.03± 3.54	77.58	8.97 ±1.92	22.42	6.06 ±1.82	0.4 ±0.05	2.51 ±0.87
11	12 Weeks	12	29.98 ± 3.23	76.68	9.12 ±1.82	23.32	6.10 ±1.62	0.5 ±0.18	2.52 ±0.92
P value			0.001	0.001	0.001	0.001	0.001	0.002	0.004

Abbreviations: (*), not detected; (--), not estimated; N, number; RS, retrosplenial.

Table 4: Labeling indices of VVA, WFA, SBA, CIC and CIC-Bodian's staining in the retrosplenial cortex of postnatal rats.

Serial N	Age	N of Animals	VVA	WFA	SBA	CIC	CIC-Bodian's
1	0 Day	6	*	*	*	*	*
2	1 Week	10	--	--	*	*	--
3	2 Weeks	10	3.60	2.94	*	*	3.52
4	3 Weeks	12	9.51	6.56	*	*	6.48
5	4 Weeks	12	12.80	8.91	1.11	2.48	8.66
6	5 Weeks	12	13.20	9.79	2.59	4.84	9.54
7	6 Weeks	12	13.95	10.69	3.86	7.23	9.97
8	7 Weeks	12	14.47	11.42	4.78	8.42	10.23
9	8 Weeks	12	14.57	11.61	6.02	8.71	10.25
10	10 Weeks	12	15.00	11.95	6.53	9.26	10.48
11	12 Weeks	12	15.84	12.82	7.43	9.87	11.02
P value			0.001	0.002	0.001	0.001	0.002

Abbreviations: (*), not detected; (-), not estimated; N, number.

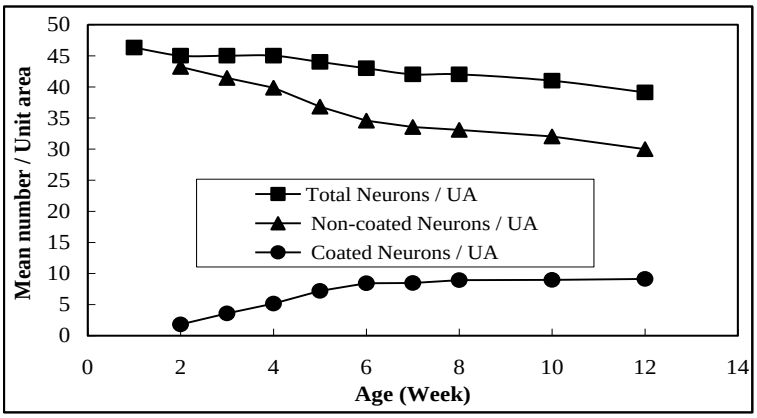
Mean number / Unit area
Age (Week)
Total Neurons / UA
Non-coated Neurons / UA
Coated Neurons / UA

2

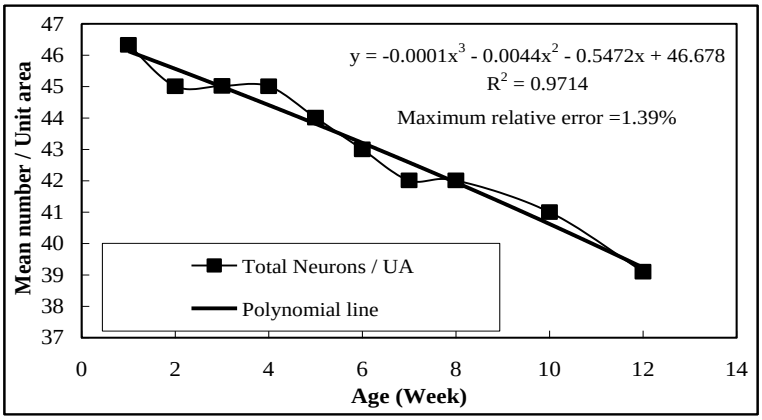
Mean number / Unit area
Age (Week)
y = -0.0001x3 - 0.0044x2 - 0.5472x + 46.678
R2 = 0.9714
Maximum relative error =1.39%
Total Neurons / UA
Polynomial line

3

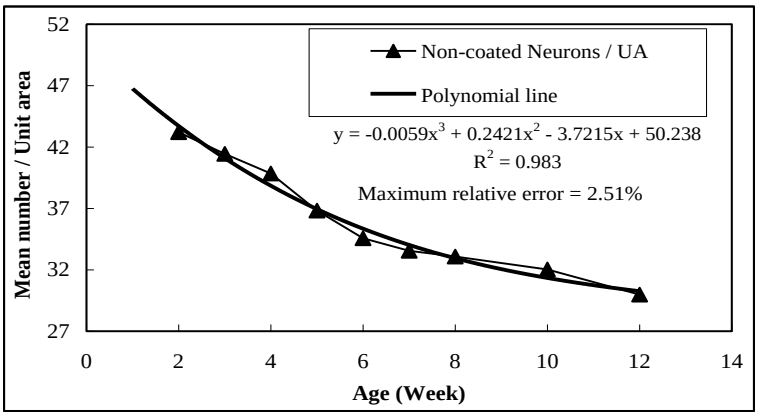
Mean number / Unit area
Age (Week)
Non-coated Neurons / UA
Polynomial line
y = -0.0059x3 + 0.2421x2 - 3.7215x + 50.238
R2 = 0.983
Maximum relative error = 2.51%

4

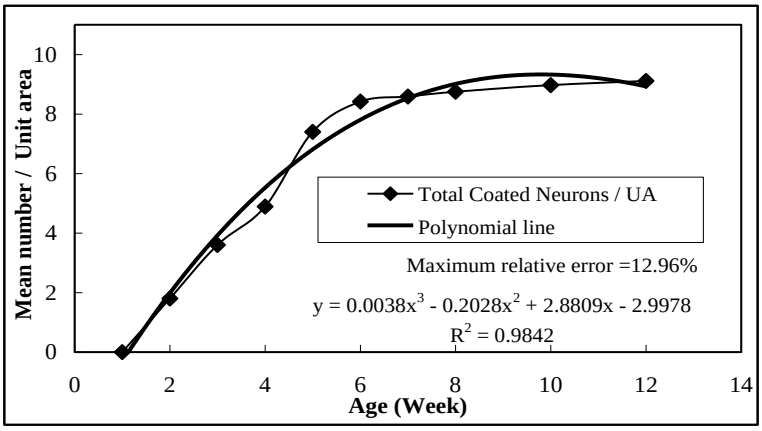
Mean number / Unit area
Age (Week)
Total Coated Neurons / UA
Polynomial line
Maximum relative error =12.96%
y = 0.0038x3 - 0.2028x2 + 2.8809x - 2.9978
R2 = 0.9842

5

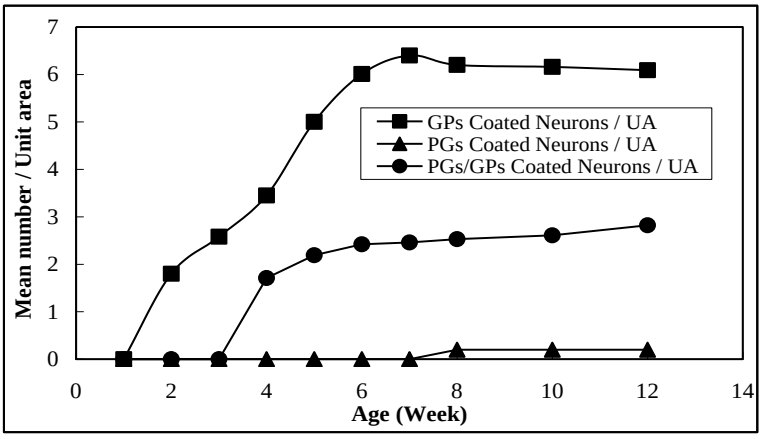
Mean number / Unit area
Age (Week)
GPs Coated Neurons / UA
PGs Coated Neurons / UA
PGs/GPs Coated Neurons / UA

6

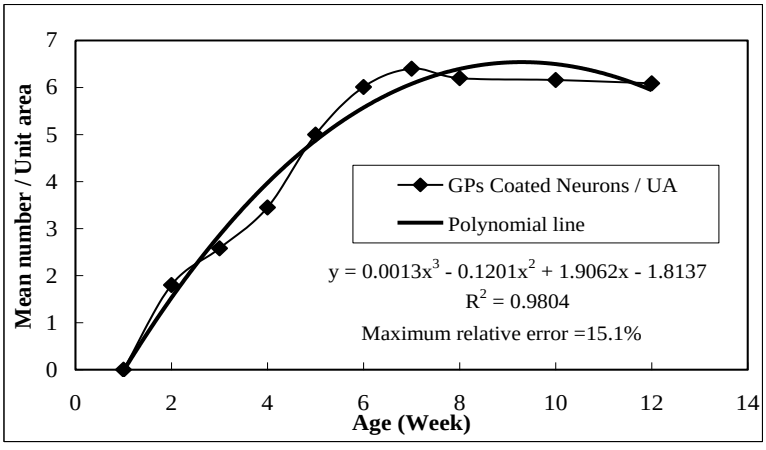
Mean number / Unit area
Age (Week)
GPs Coated Neurons / UA
Polynomial line
y = 0.0013x3 - 0.1201x2 + 1.9062x - 1.8137
R2 = 0.9804
Maximum relative error =15.1%

7

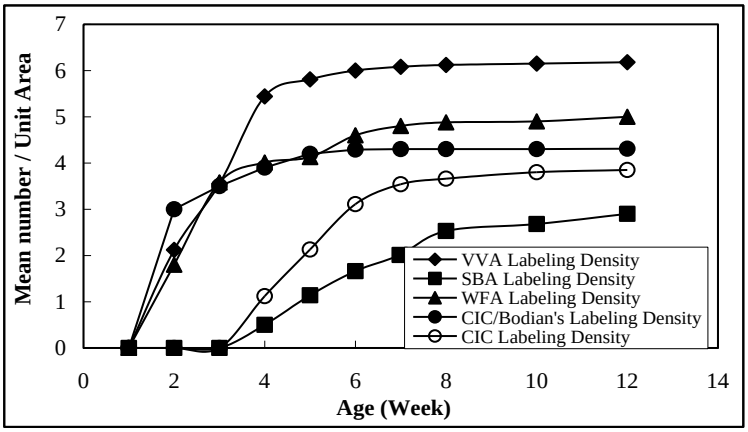
Mean number / Unit Area
Age (Week)
VVA Labeling Density
SBA Labeling Density
WFA Labeling Density
CIC/Bodian's Labeling Density
CIC Labeling Density

8

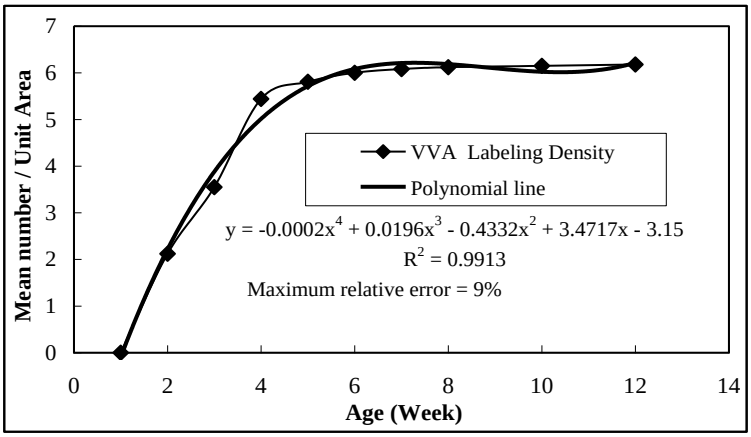
Mean number / Unit Area
Age (Week)
VVA Labeling Density
Polynomial line
y = -0.0002x4 + 0.0196x3 - 0.4332x2 + 3.4717x - 3.15
R2 = 0.9913
Maximum relative error = 9%

9

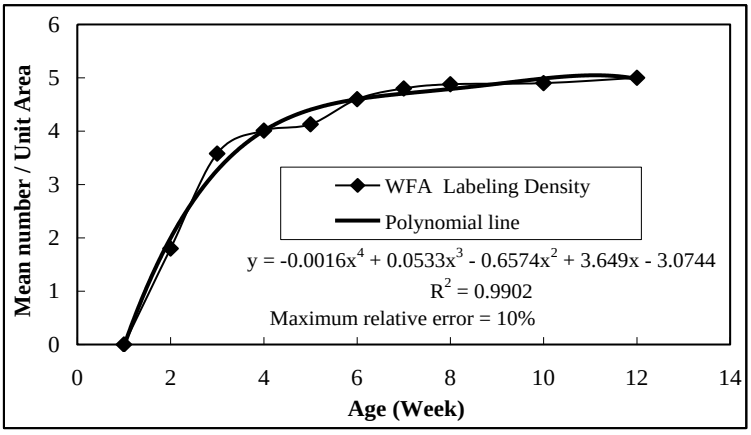
Mean number / Unit Area
Age (Week)
WFA Labeling Density
Polynomial line
y = -0.0016x4 + 0.0533x3 - 0.6574x2 + 3.649x - 3.0744
R2 = 0.9902
Maximum relative error = 10%

10

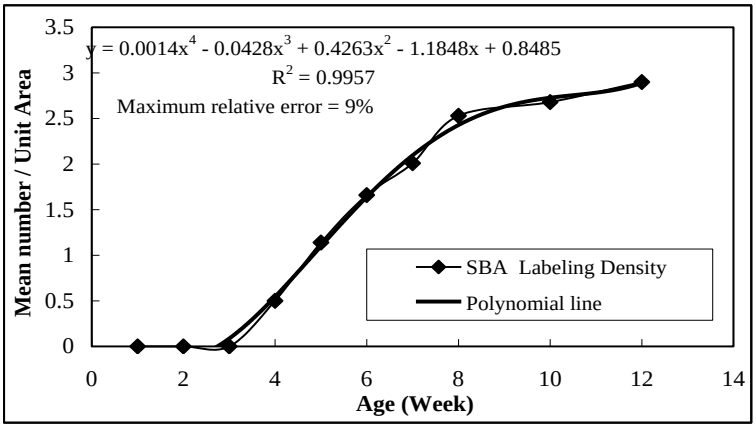
y = 0.0014x4 - 0.0428x3 + 0.4263x2 - 1.1848x + 0.8485
R2 = 0.9957
Maximum relative error = 9%
SBA Labeling Density
Polynomial line
Mean number / Unit Area
Age (Week)

11

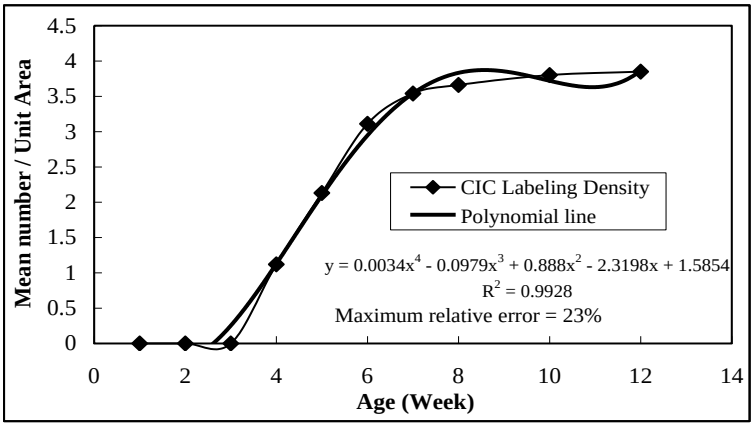
CIC Labeling Density
Polynomial line
y = 0.0034x4 - 0.0979x3 + 0.888x2 - 2.3198x + 1.5854
R2 = 0.9928
Maximum relative error = 23%
Mean number / Unit Area
Age (Week)

12

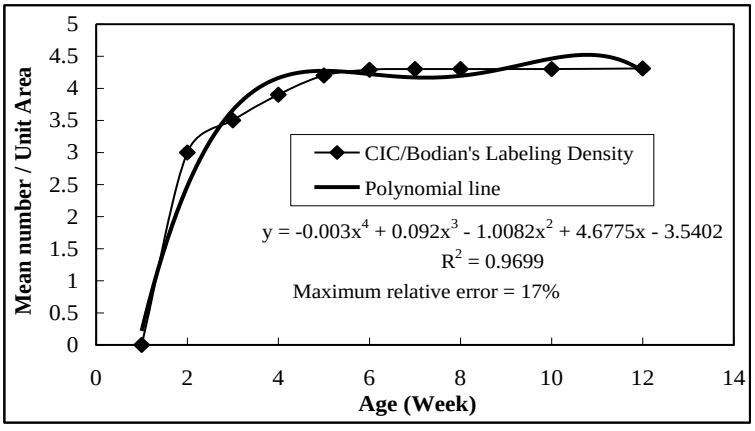
CIC/Bodian's Labeling Density
Polynomial line
y = -0.003x4 + 0.092x3 - 1.0082x2 + 4.6775x - 3.5402
R2 = 0.9699
Maximum relative error = 17%
Mean number / Unit Area
Age (Week)

13

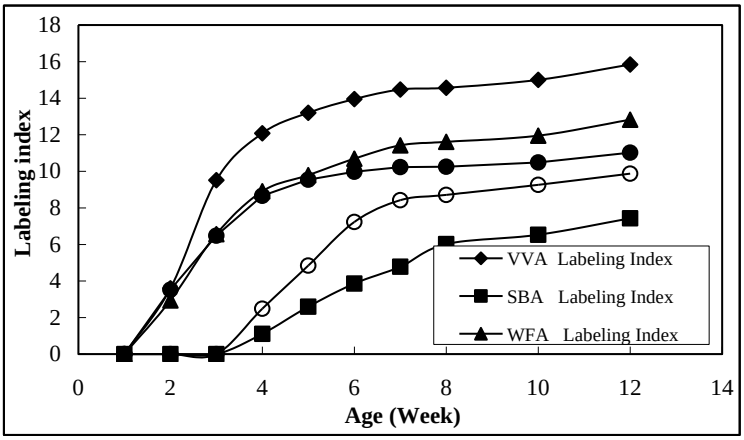
Labeling index
Age (Week)
VVA Labeling Index
SBA Labeling Index
WFA Labeling Index

14

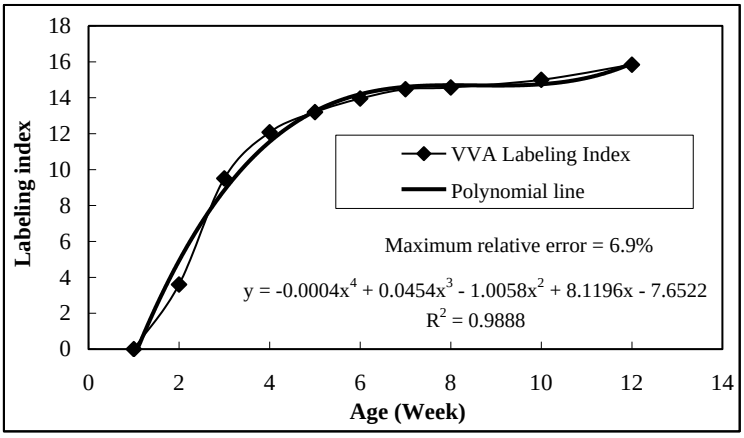
Labeling index
Age (Week)
VVA Labeling Index
Polynomial line
Maximum relative error = 6.9%
y = -0.0004x4 + 0.0454x3 - 1.0058x2 + 8.1196x - 7.6522
R2 = 0.9888

15

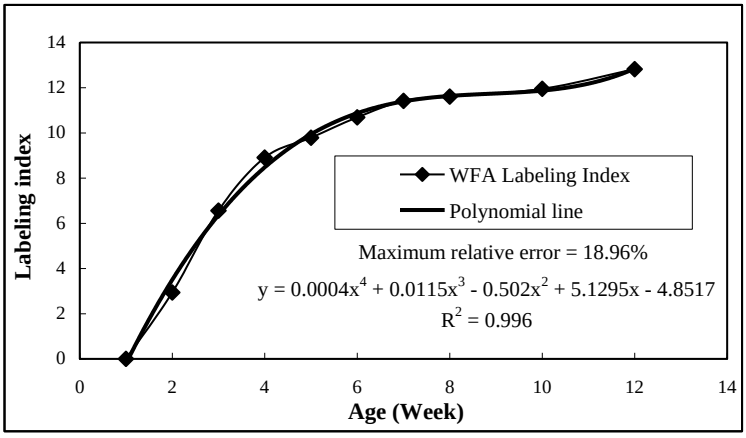
Labeling index
Age (Week)
WFA Labeling Index
Polynomial line
Maximum relative error = 18.96%
y = 0.0004x4 + 0.0115x3 - 0.502x2 + 5.1295x - 4.8517
R2 = 0.996

16

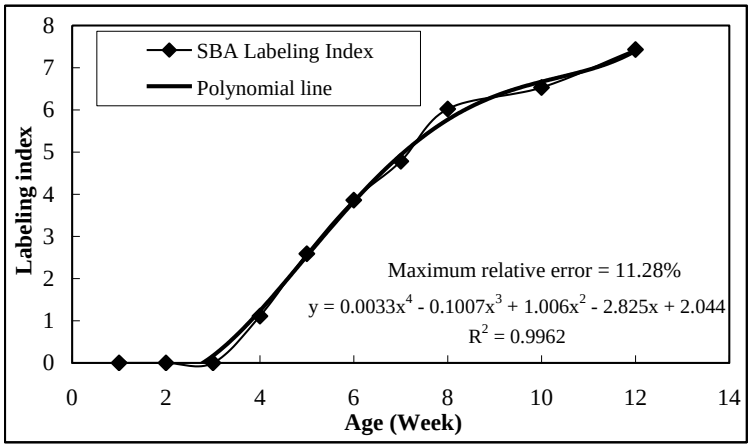
SBA Labeling Index
Polynomial line
Labeling index
Age (Week)
Maximum relative error = 11.28%
y = 0.0033x4 - 0.1007x3 + 1.006x2 - 2.825x + 2.044
R2 = 0.9962

17

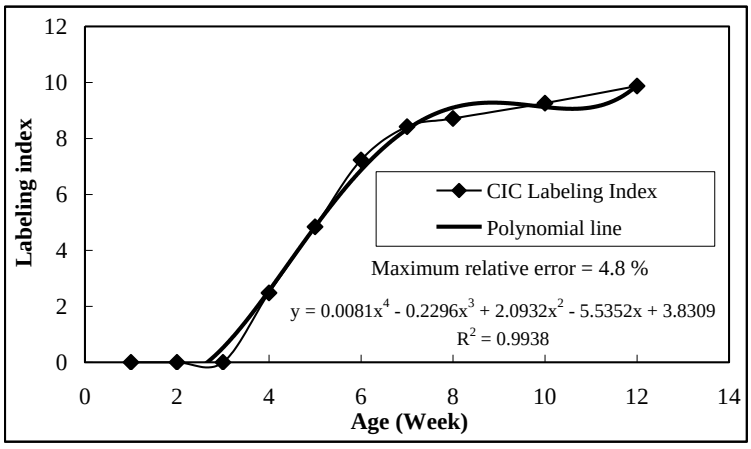
CIC Labeling Index
Polynomial line
Labeling index
Age (Week)
Maximum relative error = 4.8 %
y = 0.0081x4 - 0.2296x3 + 2.0932x2 - 5.5352x + 3.8309
R2 = 0.9938

18

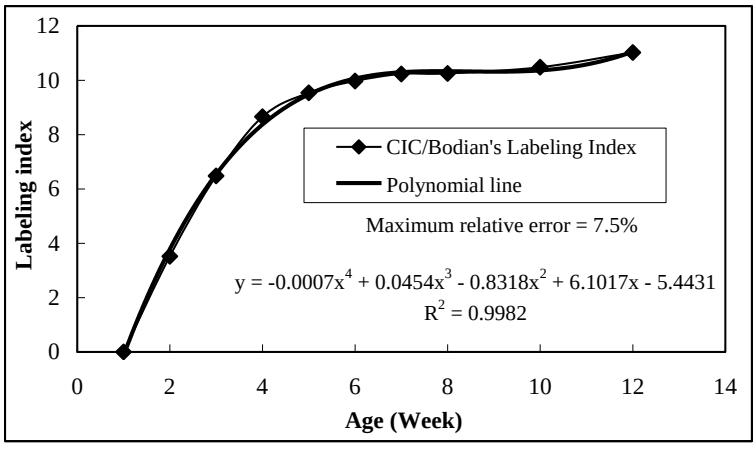
CIC/Bodian's Labeling Index
Polynomial line
Labeling index
Age (Week)
Maximum relative error = 7.5%
y = -0.0007x4 + 0.0454x3 - 0.8318x2 + 6.1017x - 5.4431
R2 = 0.9982

19

LEGENDS

Fig. 1: Survey light micrographs demonstrating the postnatal development of PNs in the RSC of rats. The differentiating net-associated neurons are distributed throughout the layers of RSC except layer I. They are most frequent in layer IV and II, but are less numerous in layers V and III. Notice, the PNs are very thin and faintly stained around pyramidal neurons (*Arrows in C*), but thick and intense around the non-pyramidal types (*Arrowheads* in A, B, C and D). I, II, III, IV & V, indicate layers of the RSC; Pw1, Pw2, Pw3 & Pw4; represent postnatal week 1, 2, 3 & 4, respectively.

A: GPs-enriched PNs. VVA-labeling countered with Meyer's hematoxyline. X33

B: PGs-enriched PNs. CIC-staining countered with nuclear fast red. X38

C: PGs-enriched PNs. CIC-Bodian's staining countered with nuclear fast red. X33

D: GPs-enriched PNs. WFA-labeling countered with Meyer's hematoxyline. X33

Fig. 2: Total neuronal density of RSNs together with the number of coated and non-coated neurons in the RSC of rats in relation to the postnatal age. The solid squares, solid circles and solid triangles equal mean that interconnected by the three irregular lines.

Fig. 3: Total numerical density of RSNs in relation to the postnatal age. The solid squares equal mean that interconnected by the thin irregular line. The thick bent line represents the best line of fit as determined by non-linear polynomial regression. The regression equation and its agreement with the data (R^2), as well as the maximum relative error are shown.

Fig. 4: Numerical density of non-coated RSNs in relation to the postnatal age. The solid triangles equal mean that interconnected by the thin irregular line. The thick bent line represents the best line of fit as determined by non-linear polynomial regression. The regression equation and its agreement with the data (R^2), as well as the maximum relative error are shown.

Fig. 5: Numerical density of coated RSNs in relation to the postnatal age. The solid rhomboids equal mean that interconnected by the thin irregular line. The thick bent line represents the best line of fit as determined by non-linear polynomial regression. The regression

equation and its agreement with the data (R^2), as well as the maximum relative error are shown.

Fig. 6: Numerical densities of GPs-, PGs- and PGs/GPs-coated RSNs in relation to the postnatal age. The solid squares, solid circles and solid triangles equal mean which are interconnected by the three irregular lines.

Fig. 7: Numerical density of glycoproteins- coated neurons in relation to postnatal age. The solid rhomboids equal mean that interconnected by the thin irregular line. The thick bent line represents the best line of fit as determined by non-linear polynomial regression. The regression equation and its agreement with the data (R^2), as well as the maximum relative error are shown.

Fig. 8: Allometric relationship between the absolute densities of VVA, WFA, SBA, CIC and CIC/Bodian's stains with the postnatal age. The solid rhomboids, solid triangles, solid circles, open circles and solid squares equal mean which are interconnected by the five irregular lines.

Fig. 9: Absolute density of VVA staining in relation to the postnatal age. The solid rhomboids equal mean that interconnected by the thin irregular line. The thick bent line represents the best line of fit as determined by non-linear polynomial regression. The regression equation and its agreement with the data (R^2), as well as the maximum relative error are shown.

Fig. 10: Absolute density of WFA staining in relation to the postnatal age. The solid rhomboids equal mean that interconnected by the thin irregular line. The thick bent line represents the best line of fit as determined by non-linear polynomial regression. The regression equation and its agreement with the data (R^2), as well as the maximum relative error are shown.

Fig. 11: Absolute density of SBA staining in relation to the postnatal age. The solid rhomboids equal mean that interconnected by the thin irregular line. The thick bent line represents the best line of fit as determined by non-linear polynomial regression. The regression equation and its agreement with the data (R^2), as well as the maximum relative error are shown.

Fig. 12: Absolute density of CIC staining in relation to the postnatal age. The solid rhomboids equal mean that interconnected by the thin irregular line. The thick bent line represents the best line of fit as determined by non-linear polynomial regression. The regression

equation and its agreement with the data (R^2), as well as the maximum relative error are shown.

Fig. 13: Absolute density of CIC-Bodian's staining in relation to the postnatal age. The solid rhomboids equal mean that interconnected by the thin irregular line. The thick bent line represents the best line of fit as determined by non-linear polynomial regression. The regression equation and its agreement with the data (R^2), as well as the maximum relative error are shown.

Fig. 14: Allometric relationship between labeling indices of VVA, WFA, SBA, CIC and CIC/Bodian's stains with the postnatal age. The solid rhomboids, solid triangles, solid circles, open circles and solid squares equal mean that interconnected by the five irregular lines.

Fig. 15: Labeling index of VVA staining in relation to the postnatal age. The solid rhomboids equal mean that interconnected by the thin irregular line. The thick bent line represents the best line of fit as determined by non-linear polynomial regression. The regression equation and its agreement with the data (R^2), as well as the maximum relative error are shown.

Fig. 16: Labeling index of WFA staining in relation to the postnatal age. The solid rhomboids equal mean that interconnected by the thin irregular line. The thick bent line represents the best line of fit as determined by non-linear polynomial regression. The regression equation and its agreement with the data (R^2), as well as the maximum relative error are shown.

Fig. 17: Labeling index of SBA staining in relation to the postnatal age. The solid rhomboids equal mean that interconnected by the thin irregular line. The thick bent line represents the best line of fit as determined by non-linear polynomial regression. The regression equation and its agreement with the data (R^2), as well as the maximum relative error are shown.

Fig. 18: Labeling index of CIC staining in relation to the postnatal age. The solid rhomboids equal mean that interconnected by the thin irregular line. The thick bent line represents the best line of fit as determined by non-linear polynomial regression. The regression equation and its agreement with the data (R^2), as well as the maximum relative error are shown.

Fig. 19: Labeling index of CIC-Bodian's staining in relation to the postnatal age. The solid rhomboids equal mean that interconnected by the thin irregular line. The thick bent line represents the best

line of fit as determined by non-linear polynomial regression. The regression equation and its agreement with the data (R^2), as well as the maximum relative error are shown.

DISCUSSION

1. General remarks

The present investigation deals with the postnatal development and quantification of PNs, as well as their course of differentiation and maturation in the RSC, which has not been morphometrically documented in rats (Sayed *et al.,* 2002, 2004). The expression of developing PGs and GPs components of PNs in the RSC was revealed as early as 1-2 weeks after birth, which follows an inside-out gradient, and attains the adult pattern at Pw6-8. Notably, at the early stages of postnatal development, the PNs components of ECM were revealed in association with neuroglia, as well as with certain types of non-pyramidal neurons and to a lesser extent with certain pyramidal cells. In addition, the differentiating ECM molecules, at the early postnatal life, exhibit a diffuse or patchy localization in neuropil.

Taken together with the previous studies, it is concluded that the basic morphological features of PNs in the RSC was largely identical, although certain heterogeneity is already revealed at the cytochemical and molecular level (Köppe *et al.,* 1997a, b; Sayed *et al.,* 2002, 2004; Mubarak *et al.,* 2008). Notably, distinct differences have been revealed among PNs with respect to the density and intensity of PGs and/or GPs molecules accumulating in the microenvironment of corresponding neuronal cells. According to their molecular composition, the developing PNs could be differentially identified, for the first time at the 5th postnatal week, into PGs coats, GPs coats as well as coat complexes that formed of PGs networks intermingling with GPs molecules (Sayed *et al.,* 2002, 2004). In line with Köppe *et al.,* (1997a) the differential accumulation of the ECM molecules, in the perineuronal spaces, is a continuous rather than a transient process, which is considered to be a key factor for the molecular determination of neuronal micromilieu (Sayed *et al.,* 2004).

2. Timing and differential maturation of PNs

The expression of PNs components of ECM visualized with lectin VVA and WFA (GCs with terminal GalNAc) or CIC-Bodian's stain (sulfated PGs) was revealed for the first time at the end of the first postnatal week in layer V, including layers V-III at Pw2, then covering

the V-II layers of RSC at Pw3. In contrast, the RSC of neonatal rats lacked neurons with surface reactivity for lectin VVA, WFA, as well as for the CIC-Bodian's staining. The lectin SBA labeling and CIC staining showed their binding activities for the first time during the fourth postnatal week. The burst of VVA, WFA and CIC-Bodian's labeling activities coincides with the onset of cytoplasmic immunoreactivity for glutamic acid decarboxylase in some populations of GABAergic neurons, which is possibly related to the onset of their functional maturation (Nakagawa *et al.,* 1987). A similar inside-out gradient of binding activity corresponding to the overall sequence of cortical maturation is also revealed with other markers (Köppe *et al.,* 1997a). Moreover, the timing of expressed ECM molecules explored by plant lectins used in this study or by using other basic dyes (e.g., CIC and CIC-Bodian's staining) coincides with the earlier findings indicated in the cortex of mouse (Nakagawa *et al.,* 1987; Murakami *et al.,* 1997), wild mouse (Brückner *et al.,* 2000), rat (Köppe *et al.,* 1997a) and cat (Hitomi *et al.,* 1997). It may be assumed that the expression of these ECM molecules, which follows the overall maturation of the cortex, may relate to the functional maturation of a subpopulation of GABAergic interneurons, as well as synaptic contacts terminating on these cells (Nakagawa *et al.,* 1987). Furthermore, the formation of cortical layers (Jackson *et al.,* 1989), the maturation of neuronal morphologies (Martin-Padilla, 1971), and the elaboration of transmitters (Voigt and De Lima, 1991) follows a similar pattern. The formation and structural maturation of PNs follows the caudorostral gradient of brain (Brückner *et al.,* 2000), roughly corresponding to the main periods of synaptogenesis and synaptic refinement as well as myelination in the brains of rats (Jacobson, 1963). The PNs appeared to be fully developed in all subcortical regions between PD21 and PD40 in the cerebral cortex of wild-mouse (Brückner *et al.,* 2000). Thus the development of fully differentiated PNs appears to indicate the acquisition of adult-like patterns of neuronal activity (Hockfield *et al.,* 1990). Notably, parvalbumin appears when the cells start to become active and reaches its maximum development at PD14 coincident with the timing of PNs (Du *et al.,* 1996).

3. Distribution and occurrence of PNs

The distribution of PNs as stained with WFA and VVA, as well as with SBA coincides with previous descriptions performed by using the same lectins, reported in rat (Härtig *et al.,* 1992; Sayed *et al.,* 2002, 2004; Mubarak *et al.,* 2004, 2008) and in other species such as mice

(Brückner *et al.,* 2000, 2003), guinea pig (Ojima *et al.,* 1998), short-tailed opossum (Brückner *et al.,* 1998) or in humans (Bertolotto *et al.,* 1991). In this investigation, the RSC of rats presents several net-associated neuronal subsets, as previously described in many areas of CNS including the cerebral cortex, the hippocampus, the thalamus, the cerebellum, the brain stem and the spinal cord (Celio and Blümcke, 1994). The net-associated neurons of present study were mainly distributed throughout the V-II layers of RSC, and that their perineuronal sheaths surrounds somata, primary dendrites and the initial axonal segments as previously described (Seeger *et al.,* 1994; Köppe *et al.,* 1997a; Pantazopoulos *et al.,* 2008).

4. Quantitative histochemical remarks of PNs

4.1. Number of net- associated neurons

In the present investigation, the total density of net-associated neurons at Pw2 was about 1.80±0.29 after labeling with WFA/CIC, and this variant increased polynomially with progression of postnatal age (R = +0.992; P<0.01) reaching 9.12±1.82 at Pw12. Mubarak *et al.,* (2008) revealed that the mean number of net- associated neurons at the RSC of adult albino rats per UA measured 9.57± 1.13 as revealed with the VVA/CIC staining, and this parameter underwent a non significant increase with age, reaching 10.90±2.62 at 12 months, and then showed a gradual decrease toward senility. The spatiotemporal pattern appears to be related to the functional maturation of individual neuronal systems, which is also evident in other developmental processes such as neurogenesis, synaptogenesis or myelination of other brain regions (Jacobson, 1963).

4.2. Percentage of net- associated neurons

The percentage of coated RSNs in rats of 2-weeks old measured about 4.28% as determined from the WFA-CIC stained sections, and this variant presented gradual increase with progression of postnatal age reaching 23.32% at Pw12. Mubarak *et al.* (2008) indicated that the percentage of net-associated neurons at the RSC of adult rats was about 24.25% as revealed with VVA/CIC staining. This variant measured 19.92% in two-month old rats, and underwent a gradual increase with advance of animal age reaching 28.53% at 12 months and declined thereafter to reach 24.66% at 18 months.

4.3. Differential expression of net-associated neurons

Investigation of the postnatal RSC of rats, at the fourth postnatal week, after using the dual WFA/CIC, VVA/CIC and SBA/CIC staining revealed three types of net-associated neurons: GPs-, PGs- and

PGs/GPs-coated neurons. The presence of three types of perineuronal coatings in the RSC of adult rats is in line with the previous findings of Mubarak *et al.,* (2008). In this investigation, the PGs-coated neurons and the GPs-coated ones, as well as those exhibiting coat complexes could be differentially identified during the second postnatal month by using the WFA-CIC double staining. These parameters showed a significant correlation with postnatal age (R = +0.996, +0.990 and +0.976, respectively; with P value <0.01 for all parameters).

4.4. Absolute labeling densities of RSNs stained with VVA, WFA, SBA, CIC or CIC/Bodian's staining

At Pw2, the absolute numerical density of RSNs labeled with VVA, WFA and CIC-Bodian's staining measured about 2.12±0.17, 1.80±0.13 and 3.00±0.18 /UA, respectively. On reaching Pw4, the numerical density of RSNs labeled with VVA, WFA, SBA, CIC and CIC/Bodian's staining is 5.44±0.94, 4.01±0.78, 0.50±0.12, 1.12±0.16 and 3.90±0.83, respectively. At Pw8, the aforementioned variants showed a gradual increment with progression of age, measuring 6.12±1.22, 4.88±1.05, 2.53±0.68, 3.66±0.78 and 4.30±1.05 /UA. On reaching Pw12, these parameters measured 6.18±1.23, 5.00±1.03, 2.90±0.69, 3.85±0.76 and 4.30±1.13 /UA, respectively. In the previous investigation of adult rats, Mubarak *et al.,* (2008) showed that the mean number of CIC and CIC/Bodian's stained PNs that enriched with PGs molecules was 4.01±0.42 and 4.43±0.37 /UA, respectively. This data indicated that the CIC/Bodian's staining of sulfated PGs presented a relatively higher labeling affinity and intensity than that shown by the CIC-staining. This is in line with Murakami *et al.,* (1997) who indicated that CIC/Bodian's stain revealed higher affinity and sharper visualization of sulfated PGs components in PNs than that indicated by the solely CIC staining. However, the mean number of neuronal cells exhibiting binding sites for lectin VVA, WFA, SBA on their surfaces measured about 6.45±0.87, 5.70±0.73 and 3.91±0.53 /UA, respectively. Therefore, the present findings together with that of previous studies indicated that the VVA and WFA staining of GPs components presented higher labeling affinity for N-acetyl-galactosamine containing GCs than that indicated by lectin SBA, which exhibits low affinity for the same epitope. This finding is in agreement with that data presented by Pantazopoulos *et al.,* (2008) who revealed a high number of WFA-labeled neurons in the amygdale.

4.5. Labeling indices of VVA, WFA, SBA, CIC and CIC/Bodian's staining

The labeling indices of neuronal cell population stained with VVA, WFA and CIC/Bodian's staining at Pw2 were 3.60, 2.94 and 3.52, respectively. On reaching Pw4, the labeling indices of neuronal cells stained with VVA, WFA, SBA, CIC and CIC/Bodian's staining were 12.80, 8.91, 1.11, 2.48 and 8.66, respectively. These parameters presented a gradual increment with advancement of postnatal age, reaching 14.57, 11.61, 6.02, 8.71 and 10.25 at Pw8. However, at Pw12, it measured about 15.84, 12.82, 7.43, 9.87 and 11.02, respectively. Mubarak *et al.* (2008) reported that in rats aging from 2-18 months, the mean value of labeling indices indicated by the VVA, WFA, SBA, CIC or CIC/Bodian's staining are 16.97%, 15.00%, 10.23%, 10.55% and 11.65% respectively. Taken together with previous investigations, the present data indicated that the CIC/Bodian's staining of PGs components in PNs presented a relatively higher labeling index than that shown by the CIC-staining (Mubarak *et al.*, 2008). In addition, the VVA and WFA staining of GPs components presented a higher labeling index than that indicated by lectin SBA. In their investigation, Lüth and co-authors (1992) revealed that 9-15% of nerve cells present in the visual cortex of adult rats have binding sites for lectin SBA.

5. Correlation between PNs and GABAergic parvalbumin neurons and Kv3.1b subunit of the potassium channel

In this investigation, the PNs are mainly associated to certain types of non-pyramidal neurons (interneurons), as well as to some pyramidal types in the RSC. As presented in the previous studies, however, the PNs are suggested to be associated with parvalbumin-immunorective GABAergic interneurons in the cerebral cortex (Kosaka and Heizmann, 1989; Härtig *et al.*, 1992; Brückner *et al.*, 1994), and certain cortical pyramidal neurons (Wegner *et al.*, 2003), as well as to projection and large motor neurons of the brain stem and spinal cord (Seeger *et al.*, 1994; Brückner *et al.*, 1994; Costa *et al.*, 2007). The parvalbumin is described as a well-established marker for PNs-bearing interneurons in CNS (Costa *et al.*, 2007). In addition, many of GABAergic neurons show immunoreactivity for parvalbumin (Härtig *et al.*, 1992; Morris and Henderson, 2000), and express the voltage-dependent potassium channel subunit Kv3.1b (Härtig *et al.*, 2001) and therefore, they have been attributed to the physiological category of fast-spiking neurons (Härtig *et al.*, 1999). In this situation, several authors have suggested that the strongly anionic microenvironment provided by

the CS-PGs component of PNs is a necessary complement of fast-firing neurons, since it may function as a local buffer for the excess potassium extruded by the cells (Brückner *et al.,* 1993; Härtig *et al.,* 1999).

6. Origin and source of ECM components

The cellular source of ECM components is a matter of contradiction. Many of CS-PGs within PNs are produced by neurons themselves, but some are made by associated glia (Carulli *et al.,* 2006). Other studies have suggested that the PGs components of PNs are derived from glial cells, meanwhile the GPs substance are essentially produced by the net-associated neuronal cells (Hitomi *et al.,* 1997; Murakamai *et al.,* 1997). Some authors indicated that the CS-PGs are produced by both net-bearing neurons and surrounding glia cells, however, HA and link proteins are produced exclusively by neurons (Carulli *et al.,* 2006). However, ECM glycoprotein Tn-R has been shown to be synthesized by oligodendrocytes (Brenneke *et al.,* 2004) or astrocytes (Gutowski *et al.,* 1999). Naegele *et al.* (1988) suggested a neuronal origin for these epitopes and in a further study (Naegele and Barnstable, 1991) noted a glial localization for the same epitopes. Furthermore, preferential or even exclusive glial localization has also been reported in an earlier investigation of mouse brain (Spicer *et al.,* 1996) and rat cortex (Lüth *et al.,* 1992). Notably, at the early phases of CNS development, there is evidence that glial cells synthesize HA (Deyst and Toole 1995). In his investigation, Zimmermann and Dours-Zimmermann (2008) suggested that the ECM components may be secreted by reactive astrocytes, oligodendrocyte precursors, microglia and eventually by meningeal cells. Taken together with the previous investigations it is concluded that the components of ECM are co-produced by the net-encapsulated neurons and associated glial cells.

7. Chemical heterogeneity of PNs

As indicated, diverse subpopulations of neurons in the RSC of present investigation can trap proteoglycans and/or glycoproteins nets on their surfaces in different proportions. Therefore, the basic components of the perineuronal coats have been demonstrated to be somewhat variable. In addition, clear differences exist between individual PNs with respect to the presence, as well as the quantity of PGs and/or GPs deposited in the microenvironment of corresponding neurons. The differential concentration of these epitopes appears to be a significant factor in the regulation of individual neuronal micromilieu (Brückner *et al.,* 1996b; Köppe *et al.,* 1997b) and suggests a definite or specific function for each type. In agreement with previous observations of

Brückner *et al.,* (1996a); Matthews *et al.,* (2002), the present data indicates that the molecular composition of PNs in rat RSC is heterogeneous.

8. Putative function of PNs

Although net-associated neurons comprise a distinct population in the RSC of rats, their anatomical or functional significance is quite uncertain. However, the histochemical and morphometric characterization of PNs, as presented in the present investigation, may provide certain information that has special significance in establishing correlations with experimental data. A whole plethora of functions has been ascribed to PNs including synapse stabilization and insulation (both chemically and electrically), prevention of neurotransmitter spillover, regulation or presenting growth factors to their receptors, ion homeostasis and protection role against oxidative stress (Celio *et al.,* 1998; Morawski *et al.,* 2004; Laabs *et al.,* 2005). CS-PGs have a variety of roles in the nervous system, including binding to molecules and blocking their action, presenting molecules to cells and axons and localizing active molecules to particular sites (Laabs *et al.,* 2005). It is possible that the main action of PGs is to bind and present various molecules which affect synaptic plasticity, dendrite growth, and axon growth (Deepa *et al.,* 2006). After damage to the nervous system, CS-PGs are the major axon growth inhibitory component of the glial scar tissue that blocks successful regeneration (Laabs *et al.,* 2005). Nevertheless, there are further roles for CS-PGs which include: neuronal maturation, generation of polyanionic ion-buffering microenvironment, maintenance of extracellular spaces and concentration of growth and inhibitory factors (Matsui *et al.,* 1999). Furthermore, the PNs may as they act as barrier-forming molecules (Laabs *et al.,* 2005) or could play a supportive or protective role, and serve as recognition molecules between certain neurons and their surrounding cells (Celio and Blümcke, 1994). During development CS-PGs pattern cell migration, axon growth pathways and axon terminations. Later in development and in adulthood CS-PGs associate with some classes of neuron and control plasticity (Carulli *et al.,* 2006; Laabs *et al.,* 2005). Other studies, however, have implicated PNs in stabilization of synaptic contacts, as well as in limitation of neuroplasticity (Hockfield *et al.,* 1990; Pizzorusso *et al.,* 2002).

Interestingly, the neurofibrillary changes or amyloid B deposits-characterizing Alzheimer's disease does not affect net-bearing neurons (Brückner *et al.,* 1999). In addition, the net-associated neurons are

suggested to be not susceptible to age related changes, as well as to abnormal or hyperphsphorylation (Härtig *et al.,* 2001). After damage to the nervous system, CS-PGs are the main components of the glial scar tissue that blocks successful regeneration (Laabs *et al.,* 2005). However, the encouraging results of previous enzymatic studies provided that the chondroitinase ABC could be used as a therapeutic drug for patients with damage to the CNS (Costa *et al.,* 2007).

In conclusion, the present investigation complement prior studies focused on PNs and give certain quantitative and developmental data that describes their expression and identify classes of neurons which frequently correspond to functional areas in the RSC. In addition, these structures appear to be an important factor in serving local demands for normal development of neuronal function concerning navigation and processing of episodic memory at this cortex.

9. Concluding remarks

In recent years considerable progress has been made in understanding the role of PNs in the CNS. Yet, many questions remain to be answered as to the mechanisms regulating the expression of CS-PGs and other ECM molecules in intact or injured CNS, their binding partners and the signaling cascades mediating their effects on neurons. However, removing CS-GAG chains or blocking their expression, possibly combined with treatments that enhance the intrinsic regenerative or plastic capabilities of adult CNS neurons, show considerable promise as a treatment to increase CNS repair after injury.

ACKNOWLEDGEMENTS

The experimental work of this study was carried out both at the Laboratories of Okayama University Medical School and Assiut University. Expenses of chemicals and experimental animals were sponsored by a Departmental research fund, Section of Human Anatomy, Graduate School of Medicine and Dentistry, Okayama University, Japan. The technical advice and cooperation of the former Mr. H. Kusano is greatly appreciated.

REFERENCES

Atoji, Y. and Suzuki, Y. (1992): Chondroitin sulfate in the extracellular matrix of the medial and lateral superior olivary nuclei in the dog. Brain Res, 585: 287-290.

Bertolotto, A.; Rocca, G.; Canave, G.; Migheli, A. and Schiffer, D. (1991): Chondroitin sulfate proteoglycan surrounds a subset of human and rat CNS neurons. J. Neurosci Res, 29: 225-234.

Bignami, A.; Asher, R. and Perides, G. (1992): Co-localization of hyaluronic acid and chondroitin sulfate proteoglycan in rat cerebral cortex. Brain Res, 579: 173-177.

Bradbury, E.J.; Moon, L.D.; Popat, R.J.; King, V.R.; Bennett, G.S.; Patel, P.N. et al. (2002): Chondroitinase ABC promotes functional recovery after spinal cod injury. Nature, 416: 636- 640.

Brauer, K.; Brückner, G.; Leibnitz, L. and Werner, L. (1984): Structural and cytochemical features of perineuronal glial nets in the rat brain. Acta Histochem, 74: 53-60.

Brenneke, F.; Schachner, M.; Elger, C.E. and Lie, A.A. (2004): Up-regulation of the extracellular matrix glycoprotein tenascin-R during axonal reorganization and astrogliosis in the adult rat hippocampus. Epilepsy Res, 58: 133-143.

Brückner, G.; Brauer, K.; Härtig, W.; Wolff, J.R.; Rickmann, M.J.; Derouiche, A.; Delpech, B.; Girard, N.; Oertel, W.H. and Reichenbach, A. (1993): Perineuronal nets provide a polyanionic, glia-associated form of microenvironment around certain neurons in many parts of the rat brain. Glia, 8: 183-200.

Brückner, G.; Bringmann, A.; Hartig, W.; Koppe, G.; Delpech, B. and Brauer, K. (1998): Acute and long-lasting changes in extracellular-matrix chondroitin-sulphate proteoglycans induced by injection of chondroitinase ABC in the adult rat brain. Exp Brain Res, 121: 300–310.

Brückner, G.; Bringmann, A.; Köppe, G.; Härtig, W. and Brauer, K. (1996a): In vivo and in vitro labelling of perineuronal nets in rat brain. Brain Res., 720: 84-92.

Brückner, G.; Grosche, J.; Schmidt, S.; Hartig, W.; Margolis, R.U.; Delpech, B.; Seidenbecher, C.I.; Czaniera, R. and Schachner, M. (2000): Postnatal development of perineuronal nets in wild-type mice and in a mutant deficient in tenascin-R. J. Comp Neurol, 428: 616–629.

Brückner, G.; Härtig, W.; Kacza, J.; Seeger, J.; Welt, K. and Brauer, K. (1996b): Extracellular matrix organization in various regions of rat brain grey matter. J. Neurocytol, 25: 333-346.

Brückner, G.; Hausen, D.; Härtig, W.; Drlicek, M.; Arendt, T. and Brauer, K. (1999): Cortical areas abundant in extracellular matrix chondroitin sulphate proteoglycans are less affected by cytoskeletal changes in Alzheimer's disease. Neurosci, 92: 791-805.

Brückner, G.; Seeger, G.; Brauer, K.; Härtig, W.; Kacza, J. and Bigl, V. (1994): Cortical areas are revealed by distribution patterns of proteoglycan components and parvalbumin in the Mongolian gerbil and rat. Brain Res, 658: 67-86.

Carulli, D.; Rhodes, K.E.; Brown, D.J.; Bonnert, T.P.; Pollack, S.J.; Oliver, K.; Strata, P. and Fawcett, J.W. (2006): Composition of perineuronal nets in the adult rat cerebellum and the cellular origin of their components. J. Comp Neurol, 494: 559–577.

Celio, M.R. and Blümcke, I. (1994): Perineuronal nets- a specialized form of extracellular matrix in the adult nervous system. Brain Res Rev, 19: 128-145.

Celio, M.R. and Chiquet-Ehrismann, R. (1993): "Perineuronal nets" around cortical interneurons expressing parvalbumin are rich in tenascin. Neurosci Let, 162: 137-140.

Celio, M.R.; Spreafico, R.; De Biasi, S. and Vitellaro-Zuccarello, L. (1998): Perineuronal nets: past and present. Trends Neurosci, 21: 510–515.

Costa, C.; Tortosa, R.; Domènech, A.; Vidal, E.; Pumarola, M. and Bassols, A. (2007): Mapping of aggrecan, hyaluronic acid, heparan sulphate proteoglycans and aquaporin 4 in the central nervous system of the mouse. J. Chemical Neuroanat, 33: 111-123.

Deepa, S.S.; Carulli, D.; Galtrey, C.; Rhodes, K.; Fukuda, J.; Mikami, T.; Sugahara, K. and Fawcett, J.W. (2006): Composition of perineuronal net extracellular matrix in rat brain. A different disaccharide composition for the net-associated proteoglycans. The J. Biol Chem, 281: 17789-17800.

Deyst, K.A. and Toole, B.P. (1995): Production of hyaluronan-dependent pericellular matrix by embryonic rat glial cells. Brain Res. Dev. Brain Res, 88: 122–125.

Du, J.; Zhang, L.; Weiser, M.; Rudy, B. and McBain, C. (1996): Developmental expression and functional characterization of the potassium-channel subunit Kv3.1b in parvalbumin-containing interneurons of the rat hippocampus. J. Neurosci, 16: 506-518.

Gutowski, N.J.; Newcombe, J. and Cuzner, M.L. (1999): Tenascin-R and C in multiple sclerosis lesions: relevance to extracellular matrix remodelling. Neuropathol Appl Neurobiol, 25: 207–214.

Härtig, W.; Brauer, K. and Brückner, G. (1992): Wisteria floribunda agglutinin-labelled nets surround parvalbumin-containing neurons. NeuroReport, 3: 869-872.

Härtig, W.; Derouiche, A.; Welt, K.; Brauer, K.; Grosche, J.; Mader, M.; Reichenbach, A. and Brückner, G. (1999): Cortical neurons immunoreactive for the potassium channel Kv3.1b subunit are predominantly surrounded by perineuronal nets presumed as a buffering system for cations. Brain Res, 842: 15–29.

Härtig, W.; Klein, C.; Brauer, K.; Schuppel, K.F.; Arendt, T.; Bigl, V. and Brückner, G. (2001): Hyperphosphorylated protein tau is restricted to neurons devoid of perineuronal nets in the cortex of aged bison. Neurobiol Aging, 22: 25-33.

Hendry, S.H.C.; Jones, E.G.; Hockfield, S. and McKay, R.D.G. (1988): Neuronal populations stained with the monoclonal antibody Cat-301 in the mammalian cerebral cortex and thalamus. J Neurosci, 8: 518-542.

Hitomi, S.; Su, W.D.; Hong, L.J.; Ohtsuka, A. and Murakami, T. (1997): Perineuronal sulfated proteoglycans and cell surface glycoproteins in the visual cortex of adult and newborn cats. Acta Med Okayama, 51: 295-299.

Hockfield, S.; Kalb, R.G.; Zaremba, S. and Fryer, H. (1990): Expressions of neural proteoglycans correlates with the acquisition of mature neuronal properties in the mammalian brain. Cold Spring Harbor Symp Quant Biol, 55: 505-514.

Jackson, C.A.; Peduzzi, J.D. and Hickey, T.H. (1989): Visual cortex development in the ferret. I. Genesis and migration of visual cortical neurons. J. Neurosci, 9: 1242-1253.

Jacobson, S. (1963): Sequence of myelinization in the brain of the albino rat. J. Comp Neurol, 121: 5-29.

Kawaguchi, Y.; Kaatsumaru, H.; Kosaka, T.; Heizmann, C.W. and Hama, K. (1987): Fast spiking cells in rat hippocampus (CA 1 region) contain the calcium-binding protein parvalbumin. Brain Res, 416: 369-374.

Köppe, G.; Brückner, G.; Härtig, W.; Brauer, K.; Härtig, W. and Bigl, V. (1997a): Developmental patterns of proteoglycan-containing extracellular matrix in perineuronal nets and neuropil of the postnatal rat brain. Cell Tissue Res, 288: 33-41.

Köppe, G.; Brückner, G.; Härtig, W.; Delpech, B. and Bigl, V. (1997b): Characterization of proteoglycan-containing perineuronal nets by enzymatic treatments of rat brain sections. Histochem J., 29: 11-20.

Kosaka, T. and Heizmann, C.W. (1989): Selective staining of a population of parvalbumin –containing GABAergic neurons in the rat cerebral cortex by lectins with specific affinity for terminal N-acetylgalactosamine. Brain Res, 483: 158-163.

Laabs, T.; Carulli, D.; Geller, H.M. and Fawcett, J.W. (2005): Chondroitin sulfate proteoglycans in neural development and Regeneration. Current Opinion Neurobiol, 15: 116-120.

Lüth, H.J.; Fischer, J. and Celio, M.R. (1992): Soybean lectin binding neuron in the visual cortex of the rat contain parvalbumin and are covered by glial nets. J. Neurocytol, 21: 211-221.

Maguire, E.A. (2001): The retrosplenial contribution to human navigation: a review of lesion and neuroimaging findings. Scand J. Psychol, 42: 225-238.

Martin-Padilla, M. (1971): Early prenatal ontogenesis of the cerebral cortex (neocortex) of the cat (Felis domestica): A Glogi study. I. The primordial neocortical organization. Z Anat Entwickl Gesch, 134: 117-145.

Matsui, F.; Nishizuka, M. and Oohira, A. (1999): Proteoglycans in perineuronal nets. Acta Histochem Cytochem, 32: 141-147.

Matthews, R.T.; Kelly, G.M.; Zerillo, C.A.; Gray, G.; Tiemeyer, M. and Hockfield, S. (2002): Aggrecan glycoforms contribute to the molecular heterogeneity of perineuronal nets. J. Neurosci 22: 7536–7547.

Morawski, M.; Brückner, M.K.; Riederer, P.; Brückner, G. and Arendt, T. (2004): Perineuronal nets potentially protect against oxidative stress, Exp Neurol, 188: 309-315.

Morris, N.P. and Henderson, Z. (2000): Perineuronal nets ensheath fast-spiking, parvalbumin-immunoreactive neurons in the medial septum/diagonal band complex. Eur J Neurosci, 12: 828–838.

Mubarak, W.; Sayed, R.; Ohtsuka, A.; Taguchi, T. and Murakami, T. (2004): Quantitative histochemical study of perineuronal nets in the retrosplenial cortex of albino rats. XXVth Cong of the EAVA, Oslo (July 28-31), Norway, p 131.

Mubarak, W.; Sayed, R.; Mubarak, H.A.; Ohtsuka, A. and Murakami, T. (2008): Histochemical and morphometric studies of perineuronal nets in the retrosplenial cortex of albino rat. Assiut Med. J., 32: 107-120.

Murakami, T.; Su, W.D.; Hong, L.J.; Piao, D.X.; Ohtsuka, A. and Seo, K. (1997): Physical- development of tissue-reacted cationic iron colloid with protein silver and Gold chloride. Okayama Igakkai Z, 109: 151-156.

Mura*kami, T.; Ohtsuka, A.; Su, W.D.; Taguchi, T.; Oohashi, T.; Murakami, T.; Abe, K. and Ninomiya, Y. (1999):* The extracellular matrix in the mouse brain: its reactions to endo-alpha-N-acetylgalactosaminidase and certain other enzymes. Arch Histol Cytol 62: 273-281.

Murakami, T.; Ohtsuka, A.; Taguchi, T. and Piao, D.X. (1995): Perineuronal sulfated proteoglycans and dark neurons in the brain and spinal cord: a histochemical and electron microscopic study of newborn and adult mice. Arch Histol Cytol, 58: 557-565.

Murakami, T.; Su, W.D.; Hong, L.J.; Piao, D.X.; Ohtsuka, A. and Seo, K (1997): Physical development of tissue-reacted cationic iron colloid with protein silver and gold chloride. Okayama Igakkai Z, 109: 151-156.

Murakami, T.; Taguchi, T.; Ohtsuka, A.; Sano, K.; Kaneshige, T.; Owen R.L. and Jones, A.L. (1986): A modified method of fine-granular cationic iron colloid preparation: its use in the light and electron microscopic detection of anionic sites in the rat kidney glomerulus and certain other tissues. Arch Histol Jap., 49: 12-23.

Naegele, J.R.; Arimatsu, Y.; Schwartz, P. and Barnstable, C.J. (1988): Selective staining of a subset of GABAergic neurons in cat visual cortex by monoclonal antibody VC1.1. J. Neurosci, 8:79-89.

Naegele, J.R. and Barnstable, C.J. (1991): A carbohydrate epitope defined by monoclonal antibody VC1.1 is found on N-CAM and other cell adhesion molecules. Brain Res, 559: 118-129

Nakagawa, F.; Schulte, B.A. and Spicer, S.S. (1986): Selective cytochemical demonstration of glycoconjugate- containing terminal N-acetylgalactosamine on some brain neurons. J. Comp Neurol, 243: 280-290.

Nakagawa, F.; Schulte, B.A.; WU, J.Y. and Spicer, S.S. (1987): Postnatal appearance of glycoconjugates with terminal N-acetylgalactosamine on the surface of selected neurons in mouse brain. Dev Neurosci, 9: 53-60.

Ojima, H.; Sakai, M. and Ohyama, J. (1998): Molecular heterogeneity of Vicia villosa-recognized perineuronal nets surrounding pyramidal and nonpyramidal neurons in the guinea pig cerebral cortex. Brain Res, 786: 274-280.

Oohira, A.; Matsui, F.; Tokita, Y.; Yamauchi, S. and Aono, S. (2000): Molecular interactions of neural chondroitin sulfate proteoglycans in the brain development. Arch Biochem Biophys, 374: 24-34.

Pantazopoulos, H.; Murray, E.A. and Berretta, S. (2008): Total number, distribution, and phenotype of cells expressing chondroitin sulfate proteoglycans in the normal human amygdale. Brain Res, 1207: 84-95.

Pizzorusso, T.; Medini, P.; Berardi, N.; Chierzi, S.; Fawcett, J.W. and MaVei, L. (2002): Reactivation of ocular dominance plasticity in the adult visual cortex. Science 298:1248-1251.

Rhodes, K.E. and Fawcett, J.W. (2004): Chondroitin sulfate proteoglycans: preventing plasticity or protecting the CNS? J Anat, 204: 33-48.

Sayed, R.; Mubarak, W.; Ohtsuka, A.; Taguchi, T. and Murakami, T. (2002): Histochemical study of perineuronal nets in the retrosplenial cortex of adult rats. Ann Anat, 184: 333-9.

Sayed, R.; Ohtsuka, A.; Mubarak, W. and Murakami, T. (2004): Postnatal development of perineuronal nets in the retrosplenial cortex of adult albino rat. XXVth Cong of the EAVA, Oslo (July 28-31), Norway.

Seeger, G.; Brauer, K.; Härtig, W. and Brückner, G. (1994): Mapping of perineuronal nets in the rat brain stained by collidal iron hydroxide histochemistry and lectin cytochemistry. Neurosci, 58: 371-388.

Spicer, S.S.; Naegele, J.R. and Schulte, B.A. (1996): Differentiation of glycoconjugates localized to sensory terminals and selected sites in brain. J. Comp Neurol, 365: 217-231.

Voigt, T. and De Lima, A.D. (1991): Serotoninergic innervation of the ferret cerebral cortex. II. Postnatal development. J. Comp Neurol, 314: 415-428.

Wegner, F.; Hartig, W.; Bringmann, A.; Grosche, J.; Wohlfarth, K.; Zuschratter, W. and Bruckner, G. (2003): Diffuse perineuronal nets and modified pyramidal cells immunoreactive for glutamate and the GABA (A) receptor alpha1 subunit form a unique entity in rat cerebral cortex. Exp Neurol, 184: 705-714.

Weber, E. (1980): Grundriß der biologischen Statistik 8. Aufl Fischer Stuttgart p 652.

Weibel, A.P.; McEchron, M.D. and Disterhoft, J.F. (2000): Cortical involvement in acquisition and extinction of trace eyeblink conditioning. Behav Neurosci, 114: 1058-1067.

Weibel, E.R. (1979): Stereological methods. Practical methods for biological morphometery. Volume I. London, New York, Toronto, Sydney, San Francisco: Academic press.

Wintergerst, E.S.; Vogt Weisenhorn, D.M.; Rathjen, F.G.; Riederer, B.M.; Lambert, S. and Celio, M.R. (1996): Temporal and spatial appearance of the membrane cytoskeleton and perineuronal nets in the rat neocortex. Neurosci Lett, 209: 173-176.

Yamaguchi, Y. (2000): Lecticans: organizers of the brain extracellular matrix. Cell Mol Life Sci, 57:276–289.

Zimmermann, D.R. and Dours-Zimmermann MT (2008): Extracellular matrix of the central nervous system: from neglect to challenge. Histochem Cell Biol, 130: 635-653.